



## Full Length Article

# *Sida cordifolia* L. fraction ameliorate renal injury, inflammation, apoptosis and gene expression on cisplatin induced acute kidney injury: Network pharmacology, *in vivo* and *in vitro* studies

Palash Mitra<sup>a,b</sup>, Sahadeb Jana<sup>a,b</sup>, Pipika Das<sup>a,b</sup>, Shrabani Pradhan<sup>b</sup>, Suchismita Roy<sup>b,\*</sup>

<sup>a</sup> Biodiversity and Environmental Studies Research Centre Affiliated to Vidyasagar University, Midnapore City College, Bhadutala, Paschim Medinipur 721129, West Bengal, India

<sup>b</sup> Nutrition Research Laboratory, Department of Paramedical and Allied Health Sciences, Midnapore City College, Kuturiya, Bhadutala, Midnapore 721129, India

## ARTICLE INFO

## Keywords:

Acute kidney injury  
*Sida cordifolia* L.  
Cisplatin  
Phytochemicals  
Oxidative stress  
Inflammation

## ABSTRACT

**Background:** Acute kidney injury (AKI) is known to involve oxidative stress, apoptosis and inflammation and becoming global health issue. *Sida cordifolia* L. is a medicinal plant having numerous pharmacological properties. The purpose of this study is to determine the presence of bioactive compounds in the chloroform fraction of *Sida cordifolia* L. (CFSC), and its effectiveness against cisplatin-induced AKI.

**Methods:** HPLC and ESI-MS studies were used to examine the presence of bioactive components in CFSC. Further network pharmacology study was done by using SwissTargetPrediction, GeneCards, and the string database. The renal protection by CFSC was investigated on cisplatin induced NRK-52E cells and *in vivo* experimentation. Cell viability by MTT assay and apoptosis parameters were performed by DAPI and AO/EB staining. Biochemical parameter was performed to evaluate renal function, protein expression and mRNA expression of related gene and histopathological analysis was done by H & E and PAS staining.

**Results:** CFSC contains Galangin, Naringenin, (-)-Epiafzelechin, Glycitein, 5,7-Dimethoxyflavanone and Sakuranetin as suggested by ESI-MS library analysis. The network pharmacology results suggest that numerous factors cause pathogenesis of AKI is complex. KEGG enrichment analysis showed the majority of pathways mentioned were closely related to various signaling pathways like ROS. Cell viability and apoptosis reported that CFSC could reduce cisplatin-treated cell death and apoptosis and the levels of kidney injury markers, inflammatory lipid peroxidation markers, and increase antioxidant markers.

**Conclusion:** CFSC could able to protect against renal injury, inflammation, and apoptosis from cisplatin-induced cytotoxicity and arrest the inflammation and signaling cascades of apoptosis.

## 1. Introduction

Acute kidney injury (AKI) is a syndrome that is defined by a sudden and irreversible loss of kidney function. The build-up of end products of nitrogen metabolism, such as blood urea nitrogen (BUN) and creatinine,

or both, and a decrease in urine output are used to diagnosis AKI. It is a condition where kidney function gradually declines and dialysis, renal replacement therapy, or kidney transplantation become necessary. There are approximately 843.6 million persons affected with kidney damage globally by several causes, such as burns, trauma, shock, nephrotoxic

**Abbreviations:** AKI, Acute kidney injury; ARE, Antioxidant response element; Bcl2, B-cell leukemia; BUN, Blood urea nitrogen; BW, Body weight; CFSC, Chloroform fraction of *Sida cordifolia* L.; CP, Cisplatin; Cys-C, Cystatin C; DPPH, 2,2-diphenyl-1-picrylhydrazyl; eGFR, Estimated Glomerular Filtration Rate; ESI-MS, Electrospray ionisation mass spectrometry; GAE, Gallic acid equivalents; GSH, Glutathione; H & E, Hematoxylin and eosin; HO-1, Heme oxygenase 1; HPLC, High performance liquid chromatography; IL-18, Interleukin-18; KIM-1, Kidney injury molecules; NF-κB, Nuclear factor kappa-light-chain-enhancer of activated B cells; NQO1, NAD(P)H dehydrogenase (quinone) 1; Nrf2, Nuclear factor erythroid 2-related factor 2; NRK-52E, Normal rat kidney; PBS, Phosphate buffer saline; RIPA, Radio immunoprecipitation assay; SC, *Sida cordifolia* L.; sCr, Serum creatinine; SOD, Superoxide dismutase; TOF, Time of flight; TPC, Total phenolic content; VC, Vehicle control

\* Corresponding author.

E-mail addresses: [pmitra664@gmail.com](mailto:pmitra664@gmail.com) (P. Mitra), [janasahadeb71@gmail.com](mailto:janasahadeb71@gmail.com) (S. Jana), [daspipika191@gmail.com](mailto:daspipika191@gmail.com) (P. Das), [shrabanutrition@gmail.com](mailto:shrabanutrition@gmail.com) (S. Pradhan), [suchismitaroy2011@yahoo.in](mailto:suchismitaroy2011@yahoo.in) (S. Roy).

<https://doi.org/10.1016/j.cpan.2025.05.001>

Received 7 March 2025; Received in revised form 28 April 2025; Accepted 6 May 2025

Available online 8 May 2025

1573-4129/© 2025 The Author(s). Publishing services by Elsevier B.V. on behalf of KeAi Communications Co. Ltd. This is an open access article under the CC BY-NC-ND license (<http://creativecommons.org/licenses/by-nc-nd/4.0/>).

drugs, cardiac surgery, major non-cardiac surgery, sepsis, and toxins. At the moment, treating the underlying causes and avoiding related consequences are the main goals of AKI care [1,2]. AKI can be caused by a multitude of drug-induced pathophysiology, cisplatin (CP), an anti-neoplastic platinum drug that is used to treat ovarian, lung, lymphoma, germ cell malignancies, and among other malignant tumors [3]. Cisplatin destroys DNA and RNA and forms protein adducts by attaching itself to nucleophilic macromolecules in cells and mitochondria. Accumulation of CP in renal proximal tubules can cause oxidative stress that produced ROS in the mitochondria. ROS generation in the mitochondria results in a direct link to phosphorylation of p38 and mitogen-activated protein kinase (MAPK) resulting in increased TNF- $\alpha$  production leading proximal tubular cell apoptosis. Furthermore, CP enhances the intracellular ROS generation by suppressing expression of antioxidant enzymes such as glutathione (GSH), superoxide dismutase (SOD), and also increases accumulation of lipid peroxidation marker like malondialdehyde (MDA). Apart from damaging DNA, CP also results in malfunctioning of cytoplasmic organelles, like mitochondria and endoplasmic reticulum, triggers apoptotic pathways which plays a key function in controlling inflammatory response which was linked to inflammation resolution, and induces a state of oxidative stress and inflammation that harm cells [4–6]. The Food and Drug Administration and the European Medicines Agency authorized different novel biomarkers like kidney injury molecules-1 (KIM-1), cystatin C (Cys-C), clusterin, and interleukin-18 (IL-18) that are used for studying nephrotoxicity [7–9]. KIM-1, a membrane protein which expressed at very low level in the healthy kidney and is present in both the extracellular and cytoplasmic portions. Following renal injury, the extracellular component can quickly cleave and enter tubule lumens that can be identified in urine [10,11]. The transcription factor nuclear factor erythroid 2-related factor 2 (Nrf2) is necessary for maintaining the antioxidant defense system. Using the antioxidant-response element (ARE), the Nrf2 protein regulates the expression of genes related to antioxidant defense against oxidative stress and drug detoxification. It is believed that activating Nrf2 is a crucial objective for compounds with cell-protective and antioxidant qualities, in which Nrf2 activates the expressions of antioxidant response element driven genes, such as heme oxygenase-1 (HO-1) and NAD(P)H quinone dehydrogenase 1 (NQO-1) [12,13]. Another study shows that in CP induced renal damage to the rats, the Nrf2 pathway increases antioxidant levels in the kidneys and blocks NF- $\kappa$ B signaling, which reduces inflammation by the effect of Sinapic acid [14]. According to a study, CP can be hazardous, causing kidney cells to undergo apoptosis and lowering B-cell leukemia (Bcl2) levels when injected. Furthermore, following cell death, the accumulation of myofibroblasts in the interstitial space may result in irreversible kidney injury or renal cell fibrosis [15,16]. As per the 2010 report by Bagshaw & Bellomo [17] Cys-C functions as an inhibitor for cysteine proteinase and belongs to a protein family which is essential for hydrolysis of many proteins and peptides within cells. It has been suggested that raised levels of Cys-C in the urine, serum, and mRNA are biomarkers for AKI, and they may in fact represent renal tubular epithelial cells damage. Clusterin is a significant glycoprotein that is elevated by epithelial cells of renal tissues of both animal and human models based on various types of cellular stress. Notably, it was shown that renal tubular epithelial and mesangial cells express clusterin in conjunction with proteinuria during glomerulopathy. Additionally, a study showing elevated clusterin expression in renal disease & nephrotoxicity models was discovered, suggesting that nephropathogenesis may be significantly influenced by clusterin [18].

Network pharmacology as a modern research technique is successfully applied to uncover complex and multitarget pharmacological processes in a range of illnesses. Bioinformatics, based techniques used in network pharmacology that are useful for researching and elucidating the mechanisms behind different pharmacological activities [19]. One could claim that network pharmacology has started to gain traction and is currently a widely employed method in the drug development process of the modern day [20].

Herbal formulations were used by early human days to the modern era for the remedy against many forms of diseases. A member of the Malvaceae family, *Sida cordifolia* Linn. (SC) is widely utilized in traditional Ayurvedic treatment. Many conditions, such as hypoglycemia, cardiovascular, arrhythmia, diabetes, dysentery, rheumatism, sciatica, and cystitis, are treated with it as a traditional remedy throughout the world. Its pharmacological actions include anti-inflammatory, analgesic, antimicrobial, and antioxidant properties [21,22]. Interestingly, pharmacological study ascertained negligible or low-toxicity effect of SC extract when administered orally on mice and exhibited good anti-inflammatory and analgesic activity [23]. Research found that in an *in vivo* model of diabetes, methanolic extract of SC is also helpful in treating hyperglycemia, cardiac heart disease, and hyperlipidemia [24]. HeLa cell lines were found to be cytotoxicity affected by SC methanol extract at 6–8  $\mu$ g/ml, and it was also efficient against phytopathogens including *Bacillus subtilis*, *Pseudomonas aeruginosa*, *Mycobacterium species*, *Enterobacter aerogenes*, *E. coli*, and *Micrococcus species* [25]. In rat model with nerve damage, whole SC extract and the aqueous fraction SC were reduced mechanical and thermal hypersensitivity by blocking nerve signaling that could be a viable alternative for treating chronic pain [21]. Aqueous extract of SC may be able to stimulate the enzyme thioredoxin-II to restore redox equilibrium, as it was able to save stress which was provided the first evidence that SC is linked to specific cellular pathways, which may be due to the synergistic effect of flavonoids and phenols [26]. In India, the root of SC is used widely as an ingredient for preparing various formulations of Ayurvedic medicines. The medicinal properties of SC are because of the presence of various bioactive phytoconstituents such as 2-carboxylated tryptamines,  $\beta$ -phenylamines, quinoline, quinazoline, indole, ephedrine, vasicinone, 5-hydroxy-3-isoprenyl flavone, 5, 7-dihydroxy-3-isoprenyl flavone, 6-(Isoprenyl)-3-methoxy-8-C- $\beta$ -D-glucosyl-kaempferol 3-O- $\beta$ -D-glucosyl [1–4]- $\alpha$ -D-glucoside, and many others [26,27]. Despite these all efficacy on various parts of the *Sida cordifolia* L, there was very preliminary study conducted for its nephroprotective properties. However, detailed studies on the effect of CFSC and its isolated compound on inhibiting the progression of chronic kidney disease are not available. Based on the phytomedicinal and ethno-botanical reports of SC, this current study focused to investigate the efficacy of chloroform fraction of *Sida cordifolia* L. (CFSC) on CP induced acute kidney injury through modulating inflammation and oxidative stress.

## 2. Materials and methods

### 2.1. Preparation of chloroform fraction of *Sida cordifolia* L.

Whole part of the plant, *Sida cordifolia* L. (Specimen No. VU/PM-01, Botanical Survey of India, Central National Herbarium, Kolkata) were washed and cut into very small pieces. After being shade-dried for 35–37 °C, the plant components were powdered using with an electrical grinder. The non-polar greasy component were then eliminated by dissolving 100 g of the plant dust for 24 h in 500 ml of hexane and after that hexane was discarded to get the grease free dust. A Soxhlet apparatus (Caltech Life Science, India) was then used to dissolve the residue in hydromethanol (4:6) for two hours. A rotating vacuum evaporator was used to evaporate the filtrate after the extracts had been run through Whatman No. 1 filter paper. Following that, extracts were further used in the fractionation and separation procedure. A Soxhlet device was then used to dissolve the hydromethanol extract in ethyl acetate for two hours. After the extraction, the filtrate was run through Whatman No. 1 filter paper and make air dried. For two hours, the ethyl acetate fraction was dissolved in 300 milliliters of chloroform in a Soxhlet apparatus. The filtrate was then dried on a rotary evaporator at 40–42 °C with lowered pressure after being filtered with Whatman No. 1 filtering paper. The chloroform fraction of *Sida cordifolia* L. (CFSC) is the term given to the dried fraction [10].

## 2.2. DPPH assay of CFSC

The capacity of the CFSC to scavenge DPPH (Cat. No # 1898–66-4, SRL, India) radicals was evaluated the DPPH free radical scavenging assay technique. The standard ascorbic acid (vitamin-C) (Cat. No. # 23006, SRL, India) and sample for this study were prepared using ethanol 0.5 ml of a 1 mmol/L DPPH in methanol was mixed to the tubes that held roughly 1 ml of prepared volumes of sample and standard. The absorbance of the test tubes was taken at 517 nm after they had been incubated for 15 min. The same quantity of DPPH in methanol was present in the blank solution. The DPPH radical scavenging activity percentage was calculated using the mentioned formula: DPPH radical scavenging activity (%) =  $\frac{A_{\text{control}} - A_{\text{standard/sample}}}{A_{\text{control}}} \times 100$  / A control.

## 2.3. Analysis of total phenolic content

The total amount of phenolic compounds was ascertained using an updated folin-ciocalteu technique. One milliliter of double-distilled water, 0.250 milliliters of folin-ciocalteu reagent.

(Cat. No # RM10822, HiMedia, India), and 0.250 milliliters of standard gallic acid in a range of concentrations were used to create the assay mixture. After that, in dark condition it was incubated for ten minutes. Later, the reaction mixture was mixed with two milliliters of distilled water and 2.5 milliliters of 7 % sodium carbonate (Cat. No # 497–19-8, HiMedia, India). After that, it was incubated in the dark at 37 °C for 90 min. Instead of using reaction mixture standards as a blank on a UV spectrophotometer (LMSP-UV1900, LABMAN, Maharashtra, India) the color absorbance at 760 nm was measured using double-distilled water. In a similar manner, the total phenolic content of the CFSC was analysed. The results were represented as mg gallic acid (Cat. No # 27645, Sigma Aldrich, India) equivalent per gram of powder for the sample and compared to standard curves [28].

## 2.4. Estimation of total flavonoids content spectrophotometric method

The colorimetric method of aluminum chloride was employed to estimation the flavonoids. 5.6 ml of fresh distilled water, 0.2 ml of 1 M potassium acetate (Cat. No # 44333, SRL, India), 3 ml of methanol and 0.2 ml of aluminum chloride (Cat. No # 23700, SRL, India), were combined with 1 ml of the sample (1 mg/ml) or standard of various concentration solutions. The absorbance of the reaction mixture was measured at 415 nm using a spectrophotometric technique against a blank and methanol used as a blank after 30 min at 37 °C. Total flavonoid containing compounds in CFSC was estimated by the equation:  $CC = \frac{cc \times VV}{mm}$  where; C = total content of flavonoid, in quercetin & apigenin equivalent, c = concentration of quercetin & apigenin established from the calibration curve in mg/ml, V = fraction volume in ml and m = weight of plant fraction in gm [29].

## 2.5. High performance liquid chromatographic analysis

The Agilent 1260 Infinity II Quaternary high-performance liquid chromatographic (HPLC) system, software, UV- wavelength set at 254 nm, & auto sampler set at 10 µL injection were used to analyze CFSC and standards quercetin (Cat. No # Q4951, Sigma Aldrich, India), apigenin (Cat. No# SMB00702, Sigma Aldrich, India) and glycitein (Cat. No # 14162, Cayman chemical company, USA). An Agilent poroshell C-18 column (Agilent, USA) was used for all chromatographic analysis, which was conducted at 35 °C and 0.5 ml/min. Acetonitrile (Cat. No # DG1DA11543, Merck, India) and methanol (1:1) are present in the mobile phase. Ten minutes was chosen as the run time. One milliliter of HPLC-grade methanol was used to dissolve one milligram of dry weight CFSC. Commercially available quercetin, apigenin and glycitein was used as a standard and prepared (1 mg/ml) using HPLC grade methanol (Cat. No # Q43637G, Thermofisher, India) as a solvent and run with

same procedure as sample. All standard and sample were filtered by 0.45 µm syringe filters (Cat. No # SF144–50NO, HiMedia, India) before injection [30].

## 2.6. Electro spray ionization- mass spectrometry (ESI-MS) analysis

ESI-MS analysis was carried out on the CFSC. A Waters Xero-G2-XS-Q-ToF time-of-flight (TOF) mass spectrometer was used for ESI-MS. With a scan range between  $m/z$  50–1800, the mass spectrometer and ESI source was run in positive ion mode. The sampling concentration and capillary voltage was set to 30 and 3 kV, respectively. Whereas the initial temperature was 100 °C, the 250 °C was desolvation temperature. Auxiliary gas pressure was 50 L/h (Ar), while nebulizing pressure of gas was 3000 L/h (N<sub>2</sub>). Before ingestion, the samples were diluted ten times using 0.1 % formic acid in water. At a flow rate of 5 µL/min, samples were immediately infused into the ESI source, and the acquisition period was one minute. Leucine, sodium formate and enkephalin were utilized as the lock-mass and calibrant, respectively. The software MassLynx was used to complete the product ion MS analysis [31].

## 2.7. Network pharmacology prediction

### 2.7.1. Acquiring targets of bioactive compound and acute kidney injury

The 2D Structure and SMILES information of bioactive compound were collected from PubChem (<https://pubchem.ncbi.nlm.nih.gov/>). SwissTargetPrediction (<http://www.swisstargetprediction.ch/>) was used to search for the target corresponding to bioactive compound. The standard gene names of target proteins were gained from string database (<https://string-db.org/>). Here, search for disease-related targets in three databases using the keyword "Acute kidney injury", including the GeneCards database (<https://www.genecards.org/>).

### 2.7.2. Construction of the PPI network and analysis

The targets associated with compounds and acute kidney injury were entered into an online Venn analysis tool (<https://bioinfo.gn.cnb.csic.es/tools/venny/>) to create Venn diagrams and obtain drug-disease intersection targets. The protein-protein interaction (PPI) network of the intersection targets was then constructed in the string database (<https://string-db.org/>). The "string.tsv" file was downloaded, and Cytoscape 3.7.2 was used to create a network of compound and AKI intersection targets. Finally, the Database for Annotation, Visualization and Integrated Discovery (DAVID) database (<https://david.ncifcrf.gov/>) was used for GO and KEGG analysis to visualize and analyse the obtained data. In addition, p values < 0.05 were set to better predict and validate biological processes and mechanisms. To obtain information on PPIs, the genes of the chosen components were submitted to STRING. The PPI network was generated using the "Homo sapiens" setting, and the medium confidence data > 0.4 was used to indicate the target protein's interaction. Proteins are represented by the network nodes, while related proteins are represented by the edge.

## 2.8. In-vitro experiments

### 2.8.1. Evaluation of CFSC in CP-treated toxicity of NRK-52E cells

Normal rat kidney (NRK-52E) cells were purchased from National Centre for Cell Sciences (NCCS), Pune, India. The cells were then cultivated at 37 °C in a 5 % CO<sub>2</sub> incubator with Dulbecco's Modified Eagle Medium (DMEM)-F12 (Cat. No # AL155, HiMedia, India), 10 % fetal bovine serum (Cat. No # RM1112, HiMedia, India), 1 % penicillin/streptomycin (Cat. No # A002A, HiMedia, India) and L-glutamine. The cells were employed for tests after being grown to 80–90 % confluency. The cells were tested for mycoplasma contamination and undergone STR analysis for cell line authentication. Then trypsinization was performed on cells that were 70–80 % confluent, and enough medium was added to deactivate the trypsin activity. Before cells counting on a using the methylene blue (Cat. No # MB257, HiMedia, India) by

haemocytometer exclusion method, the cells were centrifuged for 10–12 min at 1200 rpm, the supernatant was disposed of, and the pellet was resuspended in medium. The desired amount of cells was collected by diluting the cells in the media. The final seeding density for cell growth studies was maintained at  $10^6$  cells/well in a microtiter plate with a 96-well flat bottom. Cells were seeded for 24 h, then cell treated with cisplatin (CP) (Cat. No # PHR1624, Sigma Aldrich, USA), untreated, and simultaneously co-treatment with CP (30  $\mu$ M) & CFSC (5, 25, 50, 75, 100 & 200  $\mu$ g/ml) for another 24 h. Cell morphological examination and viability assay were conducted at 24 h after treatment. Passages 2–5 (NRK-52E) was used for all experiments.

### 2.8.2. MTT assay for NRK-52E cells viability

To identify any harmful effects of CFSC, cells were induced with different doses of CFSC. In short,  $10^6$  cells were sown into a 96-well plate. NRK-52E cells were exposed to different doses of CFSC and an untreated control was kept for a 24-hour period. After that, to each well 10  $\mu$ L of MTT (Cat. No # CCK003, HiMedia, India) solution was added, and yielding a final 0.5  $\mu$ g/ml concentration. Then, the 96 well plate were incubated for four hours with 5 %  $\text{CO}_2$  at 37 °C. Likewise the incubated period, the formazan crystals that had formed in the entire well were then dissolved with 100  $\mu$ L of DMSO (Cat. No # D8418, Sigma Aldrich, India). The absorbance was then measured at 570 nm to estimate cell viability. The following technique was used to assess the impact of CFSC at various dosages on CP-induced kidney toxicity.

### 2.8.3. Apoptotic analysis of NRK-52E cells by AO/EB and DAPI

NRK-52E cells were harvested and adjusted to  $10^6$  cells/ml and treated with CP (30 $\mu$ M), following exposed to several doses of CFSC (5, 25, 50, 75, 100, and 200  $\mu$ g/ml) for DAPI and (50, 75, 100, and 200  $\mu$ g/ml) for acridine orange (AO), ethidium bromide (EB) (AO, Cat. No # TC262; EB, Cat.No # MB071, HiMedia, India) staining. Then the cells were mixed with the AO/EB solution and kept at room temperature for 15 min, then the cells were examined under a fluorescent microscope. DAPI (Cat. No # D9542, Sigma Aldrich, India) was used to evaluate the nucleus morphology of control, CP, and CP with CFSC treated NRK-52E cells. The control and treated cells, in PBS were centrifuge at 1200 rpm for 5 min and stained with DAPI solution (1 mg/ml) and incubated for fifteen minutes at 37 °C in the dark. Fluorescence microscope (Olympus, model no. BX43F, cellSens Standard) images of the cells' nuclei were then obtained [32].

## 2.9. Acute toxicity study

The acute toxicity of CFSC was evaluated in a total of 24 rats. Six groups of all the rats were created, with four rats in each group. In accordance with OECD guideline 423, rats were then given a single dose of CFSC orally after a 24-hour fast. The dosages were 100, 200, 400, 1000, 2000 & 3000 mg/kg of body weight (bw). All the animals were monitored for diarrhea, tremor, sleep, salivations, behavioral pattern alterations, lethargy, mortality, and changes in skin and fur, eyes, convulsions, mucous membranes for up to 15 days following the dosage [33]. For additional testing, three distinct doses (100 mg, 200 mg, and 400 mg/kg of bw) were selected since no alterations or complications were seen. All methods followed animal ethics, and the method of euthanasia was as described in reference [34].

## 2.10. Selection of animals and animal experimental design

The procedures described by Jana et al. [35] were followed, however with significant alterations, during the *in vivo* experiments. The experimental study involved the selection of male albino Wistar strain rats in good health, weighing between 130 g and 150 g purchased from Saha Enterprise, Kolkata (Regd. No.: 1828/PO/Bt/S/15/CPCSEA). The cages made of polypropylene kept the animals at a constant temperature of between 24 and 26 degrees Celsius and a 12-hour dark and light

cycle was followed. To come to an end of the experiment, the animals were given unrestricted availability to water with regular pellet diet. The CPCSEA-registered Institutional Animal Ethics Committee (IAEC) of Midnapore City College (Registration number: Regd. No.: 2256/PO/Re/S/23/CCSEA) adopted the animal upkeep protocol. Thirty six rats were divided into six groups (n = 6): with each group contained six animals.

Group I is control received normal food and water, Group II served as Vehicle control (VC) receives 400 mg/kg of CFSC for 15 days. Group III is CP treat AKI group provided with one time intraperitoneal injection of CP (dissolved in saline water at 10 mg/kg bw), and Group IV to VI were orally fed with CFSC at 100, 200 and 400 mg/ kg bw/ day for 15 days followed by one time intraperitoneal injection of CP given at 10th day of experimentation. After experimentation, animals from all groups were sacrificed by carbon dioxide exposure as euthanasia method, as suggested by our IAEC. After initial 2 to 3 min of active exposure of  $\text{CO}_2$ , an additional 10.5 min of passive exposure reliably results in irreversible euthanasia for rats [34]. Following scarification, urine was collected for measuring the urinary profile, blood & kidney was collected for biochemical (BUN, sCr, GSH, SOD, MDA, KIM-1, Cys-C and IL-18 level) histopathological, protein expression and mRNA expression related studies.

### 2.11. Body weight, renal somatic index & biochemical analysis

In this experiment, change in body weight (%) was evaluated by deducting the [final body weight (g) -initial body weight (g)]/initial body weight (g)  $\times$  100. Renal somatic index (RSI) was determined by weighing both kidneys following their cleaning with an ice-cold of NaCl (0.9 %) and relative kidney weight (kidney index) were computed by following method (Kidney weight/total body weight)  $\times$  100 [5]. From blood, serum was separated and used to analyse serum creatinine (sCr), BUN and eGFR level as kidney functioning markers, super oxide dismutase (SOD), reduced glutathione (GSH) and MDA was estimated from kidney tissue for anti-oxidative events.

### 2.12. Detection of kidney injury markers

As per the instructions given by manufacturer (ELK biotechnology, Wuhan), urine samples were then analysed by ELISA (Robonik) to measure the levels of particular kidney damage indicators such as KIM-1 (Cat. No # ELK2288), IL-18 (Cat. No # ELK2270) level, and Cys-C (Cat. No # ELK9629) [6].

### 2.13. Quantitative reverse transcription polymerase chain reaction for analysis of mRNA expression

Total RNA from rat kidney tissues were extracted with TRIzol (Life Technologies). NanoDrop 2000c Bio spectrophotometer was used for the determination of mRNA concentration. For each RNA sample, 1  $\mu$ g of total RNA was reversely transcribed into cDNA using a High-capacity cDNA synthesis kit (Applied Biosystems, Foster City, CA, USA). Target gene expression for KIM-1, IL-18, Bcl2, Nrf2, clusterin, HO-1, NQO-1 and Cys-C was analysed by semi q-PCR analysis. Primer for the GAPDH was forward 5'-CGCTGGTGCTGAGTATGTCG-3' reverse 5'-CTGTGGTCATG AGCCCTCC-3', KIM-1 forward 5'-GTCTGTATTGTTGCCGAGTG-3' reverse 5'-GGTCTTGTGGAGGACTTGT-3', IL-18 forward 5'-GACTGGCTG TGACCCTATC-3' reverse 5'-TGTCTGGCACAGCTTTCTG-3', Cys-C forward: 5'-GCCTGTGCCTATCACCTCTTAT-3' reverse: 5'-CCTTCTGTCT GTCTCCTGGT-3', Clusterin forward 5'-AATGCTGTCAACGGGGTGAA-3' reverse 5'-TGGGAGCTCCTCAGCTTTG-3', Nrf2 forward 5'-TCCGGGTG TGTTTGTCCAA-3' reverse 5'-CGCCCGGAGATAAAGAGTT-3', Bcl2 forward 5'-GGAGATTGTGGCCTTCTTT-3' reverse 5'-GCCAATACGAC CAAATCCGTTGA-3', HO-1 forward 5'-GGTGA-CCCGAGACGGCTTC-3' reverse 5'-AGACTGGGCTCT-CCTTGTTC-3' and NQO-1 forward 5'-GGCAGAAGAGACTGATCGTA-3' reverse 5'-TGATGGGATTGAAGTT

CATGGC-3'. The housekeeping gene GAPDH was used to standardize the target gene's expression levels. The Gel Documentation Imaging System (Bio-Rad, Model no.1708275) was used to analyze all of the target gene expression data [10,35]. For qRT-PCR using an Agilent G8830A AriaMx system with SYBR Green (Cat. No. # 600882; LCGC life science, Hyderabad, India) detection assays. The  $2^{-\Delta\Delta CT}$  threshold approach was used to calculate the target gene expression fold change, which was then normalized to the controls [36].

#### 2.14. Densitometry analysis

Using a gel documentation system to record the DNA bands on the gel, software tools were utilized to do densitometry measurement and estimate the matching mRNA expression. ImageJ software was used to compare the band densities on the agarose gels. Together with the rectangular area of each individual band, the mean area values of the bands were displayed. The band density on an agarose gel was compared by selecting the same area for each band. The genes of interest (KIM-1, clusterin, Cys-C, Bcl2, Nrf2, HO-1, NQO-1 and IL-18) were divided by the housekeeping gene (GAPDH) and the mean density value of each band was plotted in Excel. ANOVA was used to evaluate all the data, and then a Tukey's multiple comparison test was run with the significance thresholds were set at  $p < 0.05$  ( $n = 6$ ) [37].

#### 2.15. Western blot analysis

The radio immunoprecipitation assay (RIPA) lysate had been added with fresh kidney tissue that was freshly weighed and ground up using a tissue grinder. The supernatant was obtained using a micropipette after the tissue lysate was collected and centrifuged. All the experimental rat kidney tissues were used to determine the protein content of the samples using the Lawry method. The samples were then prepared by adding  $5 \times$  gel loading dye and boiling it for four to five minutes at  $98^\circ\text{C}$ . Subsequently,  $50 \mu\text{g}$  of material per well was added, and the protein was transferred to nitrocellulose membrane (Bio-Rad, model no. 1658033FC) after being separated by SDS-PAGE (12 %) at a steady current of 320 mA for three hours. After blocking the membrane for two hours with 4 % BSA, primary antibodies such as KIM-1 (Cat. No # A2831), IL-18 (Cat. No # A16737) Bcl2 (Cat. No # A18415) (Abclonal, USA),  $\beta$ -actin (Cat. No. # AF7018), and Nrf2 (Cat. No. # AF0639), (Affinity Biosciences, USA) were added at a 1:1000 ratio. The membrane was then incubated by Rocker-Shaker at  $4^\circ\text{C}$  for the entire night. After four PBST washes, the membranes were incubated for two hours at room temperature with HRP conjugated secondary antibody 1:7500 (Cat. No. # 3822, AbgeneX, Bhubaneswar, India). After that, 3,3'-Diaminobenzidine (DAB) stain (Cat. No. # MB121, HiMedia, India) was used to identify the bands and then Image J software was used for densitometric analysis [38].

#### 2.16. Histopathological examinations

Before being rinsed with ice-cold saline water, the rats' kidney tissues were preserved in a 10 % formalin solution for a whole day. The kidney tissues were subjected to treatment by xylene permeabilization, gradient dehydration of alcohol, and standard processing before being embedded in paraffin and sectioned at a thickness of  $5 \mu\text{m}$ . After staining the sections with hematoxylin and eosin (H&E) and periodic acid Schiff (PAS), the sections were inspected histopathologically under a light microscope to check for congestion, inflammatory cell infiltration, or necrosis. The injured glomerular and renal tubules, including brush border, tubule dilatation, and cast formation, relative to the total number of renal tubules was used to grade renal morphology. Histological studied was performed by randomized selection of kidney tissue section [10]. An expert in renal pathology blindly inspected these portions. On a five-point scale based on the extent of involvement, the proportion of histological alterations in the cortex and medulla were assessed using a semiquantitative approach intended to assess the degree of necrosis, cell

loss, and necrotic casts: 0.5, less than 10 %; 1, 10–25 %; 2, 25–50 %; 3, 50–75 %; and 4, 75–100 %; 0, normal kidney [39].

#### 2.17. Determine the nuclear DNA morphological assessment using DAPI staining

Fresh kidney tissue (50 mg) samples were washed with phosphate-buffered saline (PBS), then added in 0.5 ml (2 mg/ml) collagenase (Cat. No # TC211, HiMedia, India) mixed with PBS and mince the tissue using a sharp scalpel. Samples were then filtered by using a nylon filter mesh ( $20 \mu\text{m}$ ). After that,  $20 \mu\text{L}$  of the samples were smeared on a grease-free slide and dried under laminar air flow. The slide was then fixed with chilled methanol, and after that, the slide was washed with 4 % paraformaldehyde (Cat. No # TC703, HiMedia, India). DAPI stain (1:1000) was used to observe the changes in the nuclear morphology and visualized by fluorescence microscope (Olympus, model no. BX43F, cellSens Standard) and apoptotic cells count by ImageJ software.

#### 2.18. Statistical analysis

Statistical analysis for all measured parameters were performed using the GraphPad Prism 8.0.1 statistical software package. Differences among experimental groups were assessed by two-way ANOVA analysis followed by Tukey's multiple comparison test. Data were presented as means  $\pm$  SE. Values were considered significantly different when ( $p < 0.05$ ).

### 3. Results

#### 3.1. Estimation of total phenolic and flavonoids content

Total content of phenolic compounds of CFSC was expressed as gallic acid equivalents (GAE), total content of flavonoid compounds were expressed as quercetin and apigenin using the standard curve equation. This fraction contains a very good amount of phenolic and flavonoids content as shown in Table 1.

#### 3.2. DPPH radical scavenging assay

The antioxidative potentiality of CFSC and the standard (vitamin C) were measured depending on the free radical scavenging activity of stable 1,1-diphenyl-2-picrylhydrazyl (DPPH) radical. The percentage values of CFSC was  $72.0525 \pm 2.182827$ , whereas for standard vitamin C it was  $91.3525 \pm 1.274336$  (Table 2).

#### 3.3. HPLC analysis of CFSC

The HPLC fingerprints of CFSC (Fig. 1A) has shown three major and many minor peaks area at the wavelength of 254 nm. CFSC showed major and minor peak area at the retention time (RT) 2.621, 2.891,

**Table 1**  
Total phenolic and flavonoid contents of CFSC.

Name of fraction	TPC (mgGAE/g)	TFC	
		mg quercetin/g	mg apigenin/g
CFSC	$2.43 \pm 0.63$	$1.517 \pm 0.355$	$1.506 \pm 0.481$

**Table 2**  
DPPH radical scavenging activity of CFSC using standard ascorbic acid.

Name of fraction & Standard	DPPH%
CFSC	$72.0525 \pm 2.182827$
Ascorbic acid	$91.3525 \pm 1.274336$

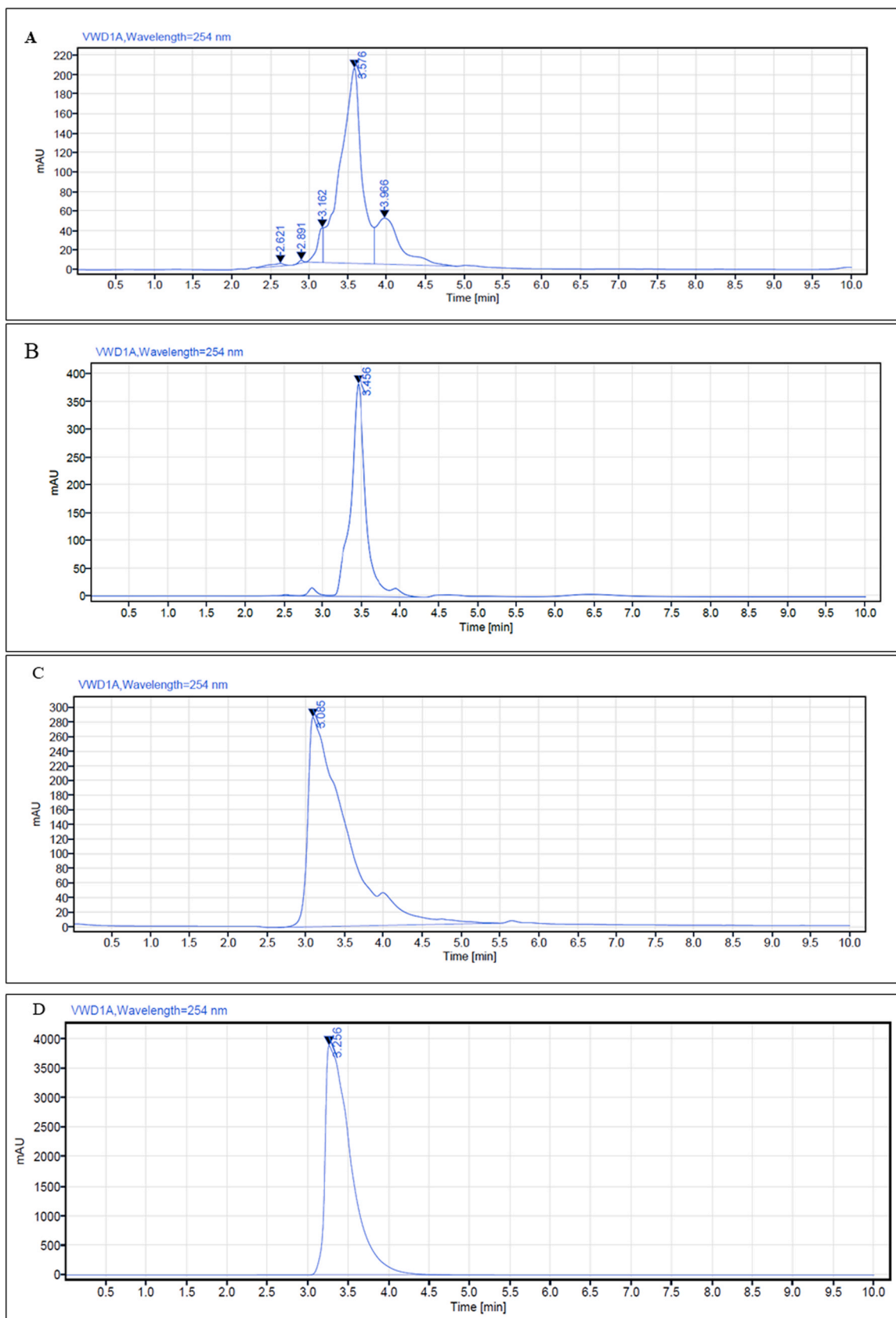


**Fig. 1.** HPLC analysis of chloroform fraction of *Sida cordifolia* L. at 254 nm (1A), HPLC analysis of standard quercetin at 254 nm (1B), HPLC analysis of standard apigenin at 254 nm (1C) and HPLC analysis of standard glycitein at 254 nm (1D).

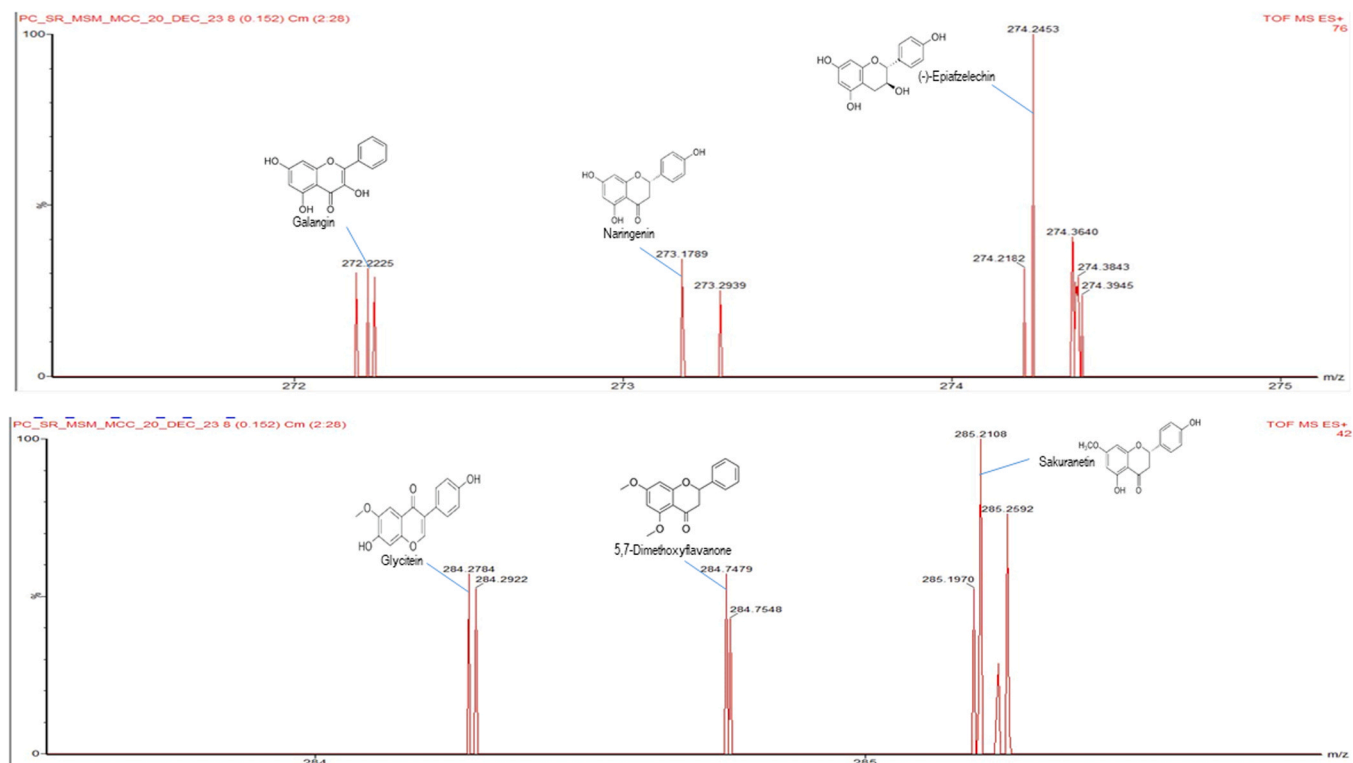


Fig. 2. ESI-MS chromatogram of chloroform Fraction of *Sida cordifolia* L.

3.162, 3.576 and 3.966 against compared to standards compound like quercetin (Fig. 1B), apigenin (Fig. 1C) and glycitein (Fig. 1D) RT 3.456, 3.085 and 3.256.

#### 3.4. ESI-MS profiling of the CFSC

The ESI-MS profiling of the CFSC was done for identification and characterization of the bioactive compounds probably present in this plant using Mass Bank library by MassLynx software. A total of 6 compounds including Galangin, Naringenin, (-)-Epiatzelechin, Glycitein, 5,7-Dimethoxyflavanone and Sakuranetin from the library was possibly identified in the chloroform fraction along with their  $m/z$  value (Fig. 2 & Table 3).

#### 3.5. Effects of bioactive compounds on AKI were explored based on network pharmacology

Absorption, distribution, metabolism, and excretion (ADME)-related information of bioactive compounds including Galangin, Naringenin, (-)-Epiatzelechin, Glycitein, 5,7-Dimethoxyflavanone and Sakuranetin were searched by SwissADME (<http://www.swissadme.ch/>) (Table 4). The network pharmacology method was used to identify the relevant targets and pathways of compounds in the treatment of AKI. These results suggest that numerous factors cause pathogenesis of AKI is complex. Gene datasets obtained from the screening of AKI targets and compounds (Galangin, Naringenin, Glycitein, 5,7-Dimethoxyflavanone and Sakuranetin)-related targets were imported into an online Venn diagram, and a total of 467 intersecting targets were obtained (Fig. 3A-E). Fig. 3F Venn diagram showed that after the all compound targets were normalized and the duplicate values were removed, total of 243 intersecting targets were obtained. To obtain the compound target network, the intersection targets were imported into the string database (Fig. 4A). The graphs were generated using Cytoscape 3.7.2 software (Fig. 4B). Functional bioinformatics analysis found the biological processes (BP), cellular component (CC), and molecular function (MF)

consisted of 653, 100, and 243 items, respectively. BP analysis showed that most of these targets are closely related to the regulation of chromatic remodeling, signal transduction, protein phosphorylation, inflammatory response, apoptotic process, positive regulation MAPK cascade, positive regulation of gene expression (Fig. 5A). CC analysis indicated that these targets were distributed in the plasma membrane, cytosol, nucleus, cytoplasm, extra cellular space, mitochondria, Golgi apparatus, endoplasmic reticulum (Fig. 5B). MF analysis revealed that these targets were associated with protein binding, ATP binding, enzyme binding, protein serine/threonine kinase activity, kinase activity (Fig. 5C). KEGG enrichment analysis suggests that the majority of pathways mentioned here are closely related to metabolic pathway, chemical carcinogenesis ROS, MAPK and cAMP signaling pathway, RAS signaling pathway (Fig. 5D). The results show that metabolic pathway and oxidative stress are all involved in bioactive compounds preventing AKI.

#### 3.6. Effect of CFSC on CP-treated toxicity in kidney cells

The efficacy of CFSC in CP-treated cytotoxicity in NRK-52E cells was evaluated using the MTT test. Cell viability was evaluated in order to ascertain the cytoprotective effect of CFSC in CP-treated NRK-52E cells. NRK-52E cells were exposed to several doses of CFSC during a 24-hour period at dosages of 5, 25, 50, 75, 100, and 200  $\mu\text{g}/\text{ml}$ , either alone or in combination with CP (30  $\mu\text{M}$ ). Treatment with CFSC alone did not negatively impact the viability of NRK-52E cells (Fig. 6A). CFSC treatment significantly improved the vitality of CP-induced NRK-52E cells. It was found that the  $\text{EC}_{50}$  was 25.12  $\mu\text{g}/\text{ml}$  (Fig. 6B). Treatment of CP significantly ( $P < 0.001$ ) reduced the viability of NRK-52E cells with compared to Control NRK-52E cells.

#### 3.7. Effect of CFSC on apoptosis of kidney cell line

NRK-52E cells were stained with DAPI and AO/EB, and their apoptotic nature was then observed under a fluorescence microscope.

**Table 3**  
List of possible bioactive compounds present in CFSC as analyzed by TOF-ESI-MS study.

Sl. No.	Mass <i>m/z</i>	Ionization mood	Name of suggested compounds	Molecular formula	Pharmacological activities
1.	272.22	[M + H] <sup>+</sup>	Galangin	C <sub>15</sub> H <sub>10</sub> O <sub>5</sub>	It effectively reduces nephrotoxicity by inhibiting ERK and NF-κB signaling pathways, reducing oxidative stress, inflammation, and cell death [40].
2.	273.17	[M + H] <sup>+</sup>	Naringenin	C <sub>15</sub> H <sub>12</sub> O <sub>5</sub>	It may protective effects on nephrotoxicity by increasing antioxidant enzymes [41] and also antidiabetic effect [42].
3.	274.24	[M + H] <sup>+</sup>	(-)-Epiafzelechin	C <sub>15</sub> H <sub>14</sub> O <sub>5</sub>	It reduces lipid peroxidation, which decrease DNA damage [43]. Also inhibited SARS-CoV-2 replication or transcription by binding to the 3C <sub>pro</sub> and RdRp viral proteins [44].
4.	284.27	[M + H] <sup>+</sup>	Glycitein	C <sub>16</sub> H <sub>12</sub> O <sub>5</sub>	It improved the anti-stress capabilities of nematodes and activated the antioxidant defence system [45]. It additionally mitigates lipid peroxidation and inflammatory stress [46].
5.	284.75	[M + H] <sup>+</sup>	5,7-Dimethoxyflavanone	C <sub>17</sub> H <sub>16</sub> O <sub>4</sub>	It has antioxidant, anti-inflammatory properties which helps to prevent acute toxicity as well as gastric ulcer [47], anticancer activity [48].
6.	285.21	[M + H] <sup>+</sup>	Sakuranetin	C <sub>16</sub> H <sub>14</sub> O <sub>5</sub>	It may prevent inflammatory and oxidative stress related gastric ulcer [49], also improved osteoarthritis by inhibiting the PI3K/AKT/NF-κB pathway [50], its help to protect nephrotoxicity [51].

**Table 4**  
ADME analysis of bioactive compounds for pharmacokinetics and druglikeness properties.

Compound's	Pharmacokinetics										Druglikeness	
	GI absorption	BBB permeant	P-gp substrate	CYP1A2 inhibitor	CYP2C19 inhibitor	CYP2C9 inhibitor	CYP2D6 inhibitor	CYP3A4 inhibitor	Log Kp (skin permeation)	Lipinski	Bioavailability Score	
Galangin	High	No	No	Yes	No	No	Yes	Yes	-6.35 cm/s	Yes	F > 10 %	
Naringenin	High	No	Yes	Yes	No	No	No	Yes	-6.17 cm/s	Yes	F > 10 %	
(-)-Epiafzelechin	High	No	Yes	No	No	No	No	No	-7.46 cm/s	Yes	F > 10 %	
Glycitein	High	No	No	Yes	No	No	Yes	Yes	-6.30 cm/s	Yes	F > 10 %	
5,7-Dimethoxyflavanone	High	Yes	No	Yes	Yes	Yes	Yes	Yes	-5.92 cm/s	Yes	F > 10 %	
Sakuranetin	High	Yes	No	Yes	Yes	No	No	Yes	-6.02 cm/s	Yes	F > 10 %	

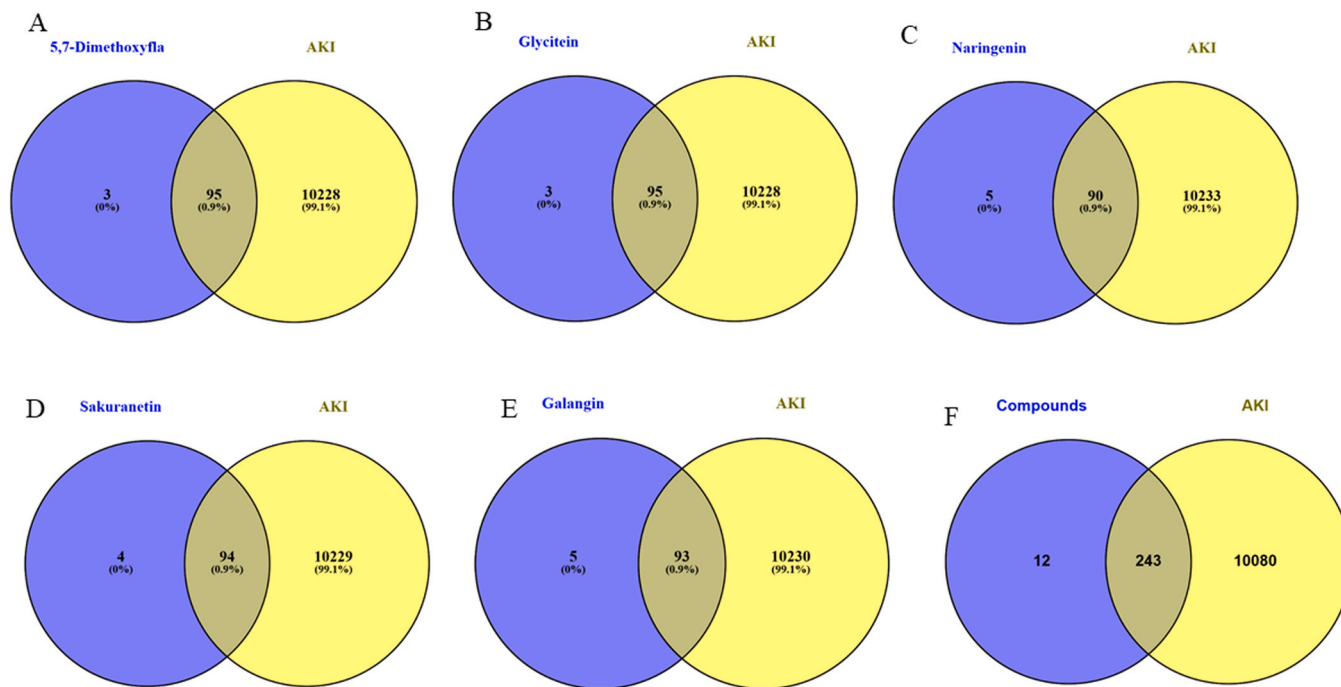


Fig. 3. Venn diagram of the intersection target between AKI and compounds.

DAPI staining showing nuclear morphology of the CP and CFSC treated NRK-52E cells (Fig. 7A-I). CP led to cell apoptosis as indicated by its tendency to induce cell shrinkage, chromatin condensation and nuclear fragmentation. Similarly, AO/EB staining showed that the control group has green living cells with normal morphology (Fig. 7J). Whereas cells treated with CP at a dose of 30uM, nuclear disintegration, membrane blebbing, and cell shrinkage were noted. These cells at early apoptotic stage was observed with green chromatin condensation, while the nucleus of late apoptotic stage stained with orange that included fragmented DNA with beads (Fig. 7K). Different concentrations of CFSC were added to CP-treated cells, resulting in the appearance of living cells with distinct chromatin and bright green nucleus structures (Fig. 7L-O) that indicate decrease apoptotic cells due to treatment of CFSC.

3.8. Effect of CFSC on body weight and kidney somatic index on CP induced AKI

Each experimental animal's initial body weight (Fig. 8A) and final body weights were noted. As illustrated in Fig. 8B & C, the CP-treated rats exhibited a significant ( $p < 0.05$ ) reduction in body weight percentage and increased in renal somatic index in comparison to the control group. In rats treated with high doses of CFSC (200 and 400 mg/kg bw), the renal somatic index reduced and the body weight increased significantly ( $p < 0.05$ ) in comparison to rats treated with CP-induced AKI. However, the lower dose i.e. 100 mg/kg bw of CFSC was not effective and so could not be able to maintain the normal body weight.

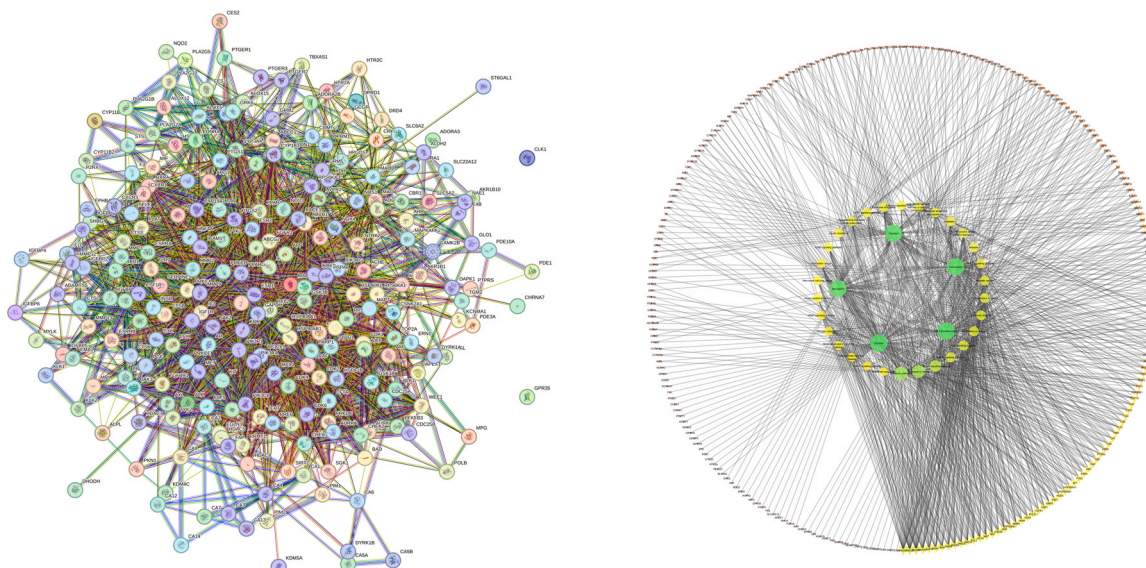


Fig. 4. PPI network with 243 intersecting targets using string database (A) and Cytoscape (B).

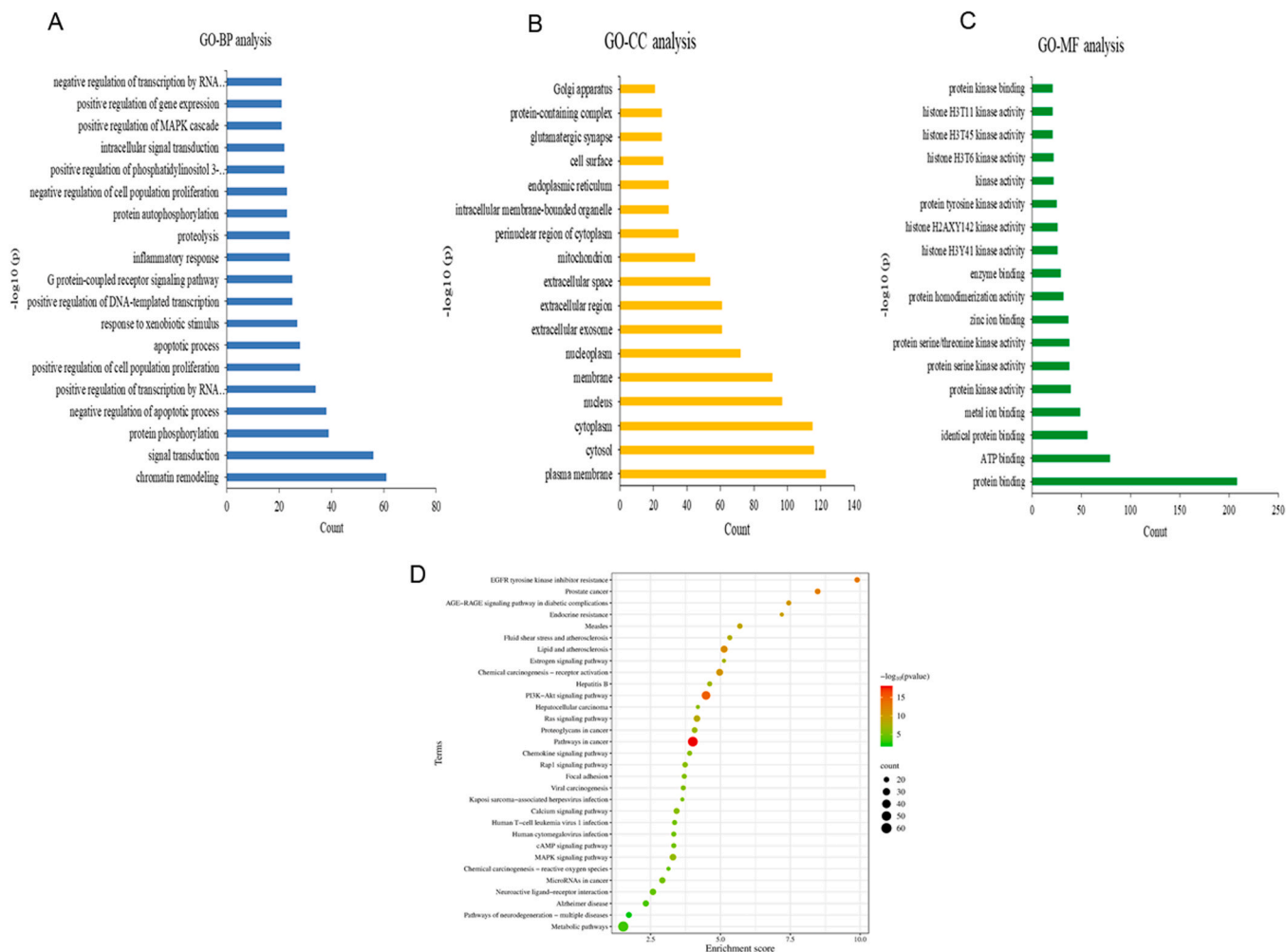


Fig. 5. GO and KEGG functional analysis. Diagram of GO-BP analysis (A); GO-CC analysis (B); and GO-MF analysis (C); KEGG pathway enrichment analysis (D).

### 3.9. CFSC improves renal function in CP induced AKI

Blood urea nitrogen (BUN) and sCr levels were significantly ( $p < 0.05$ ) increased and the eGFR level was significantly decreases in the CP-treated animals compared to control group, as shown in Fig. 9A-C. BUN, sCr, and eGFR levels were considered to be the key indicators of kidney injury including CP induced AKI [10,35]. This suggested that

CP induced toxicity resulted impaired renal functioning and an abnormal level of kidney injury markers were observed. The CP treated rats receiving CFSC orally at 200 and 400 mg/kg bw/day for 15 days showed a significant ( $p < 0.05$ ) decrease in these traditional indicators of kidney damage due to presence of bioactive compounds in CFSC and their nephroprotective properties. CP treated animals orally fed with CFSC at the lower dose i. e. 100 mg/kg bw was unable to offer

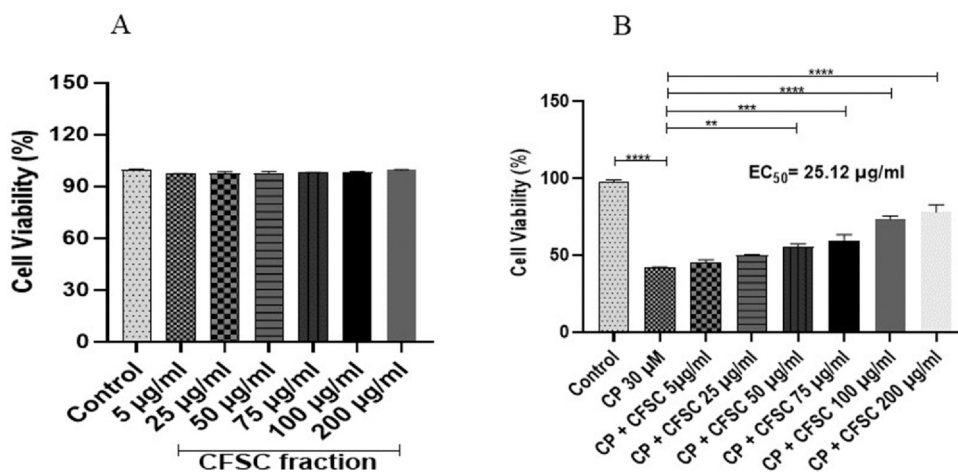
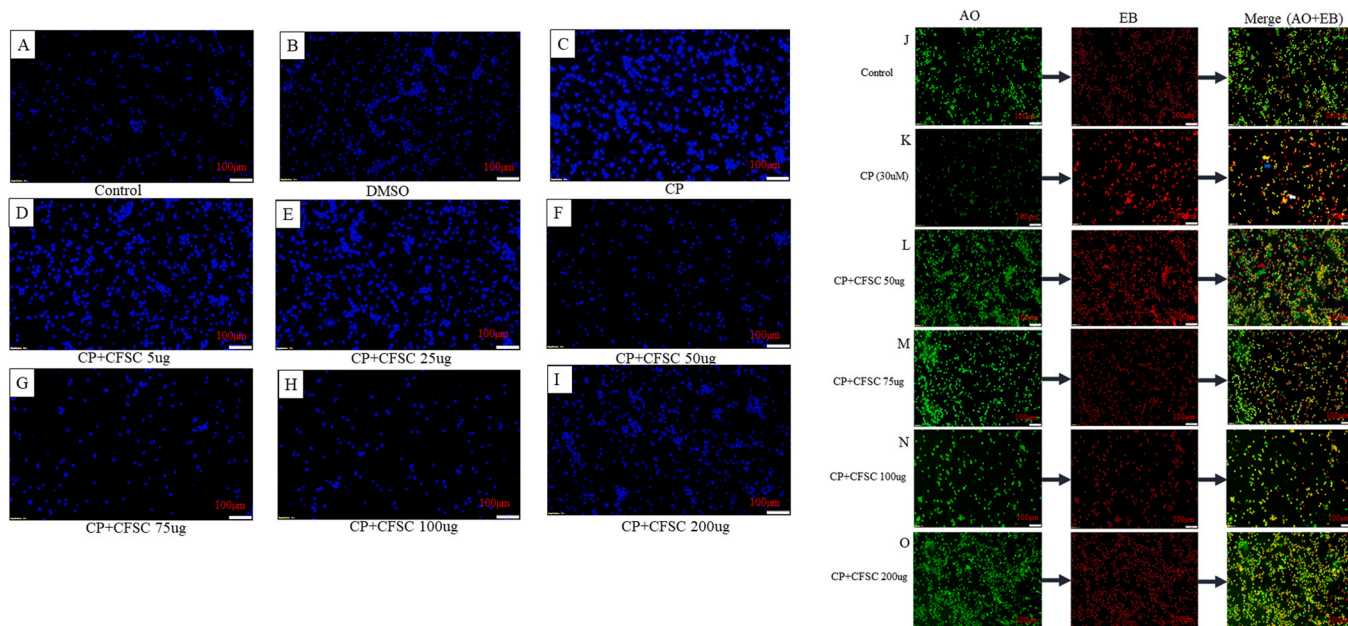


Fig. 6. Cell viability test of CFSC (A), and CP with CFSC treated on NRK-52E cells (B). Data were expressed as Mean  $\pm$  SE ( $n = 3$ ). Statistical analysis of two-way ANOVA followed by Tukey's multiple comparison test were performed and significance level was tested at  $**p < 0.01$ ,  $***p < 0.001$ ,  $****p < 0.0001$ .



**Fig. 7.** Apoptotic study of NRK-52E cells using the fluorescence microscopy after staining with DAPI (A-I) & AO/EB (J-O) staining on NRK-52E cells treated with CP and CFSC at different concentrations. Early apoptotic cells exhibit bright green nuclear margination and chromatin condensation, while green live cells display normal nucleus morphology. Apoptotic structures and fragmented orange chromatin were seen in late apoptotic cells. Yellow arrows indicate viable cells, blue arrows indicate early apoptotic cells, and white arrows indicate late apoptotic cells.

nephroprotection and thereby fails to maintain normal levels of BUN, sCr, and eGFR.

**3.10. Effect of CFSC on the antioxidant and lipid peroxidation activities of CP induced AKI**

In comparison to the control group, the GSH and SOD levels were significantly ( $p < 0.05$ ) lower in the kidney tissues of the CP-induced nephrotoxic rats. In contrast, CP treated rats provided with CFSC at high dosages (200 mg and 400 mg/kg bw/day) for 15 days showed a markedly ( $p < 0.05$ ) elevated level of these antioxidants in their kidneys. The MDA content in group III rats was substantially higher ( $p < 0.05$ ) after CP treatment than in the control group. Conversely, the overproduction of MDA was considerably reduced when CFSC was

orally fed at the doses of 200 and 400 mg/kg bw ( $p < 0.05$ ) (Fig. 10A, B and C).

**3.11. Effect of CFSC on the anti-inflammatory activities on CP induced AKI**

This study used ELISA to assess the production of inflammatory cytokines in urine. According to the results, animals in group III that received CP treatment had considerably ( $p < 0.05$ ) higher urine levels of KIM-1, IL-18, and Cys-C than the control group. Significantly ( $p < 0.05$ ) lower levels of these urine biomarkers were seen after 15 days of treatment with high doses of CFSC, i.e., 200 and 400 mg/kg bw/day, which preserved the tubular structural integrity and prevented inflammation (Fig. 11A-C).

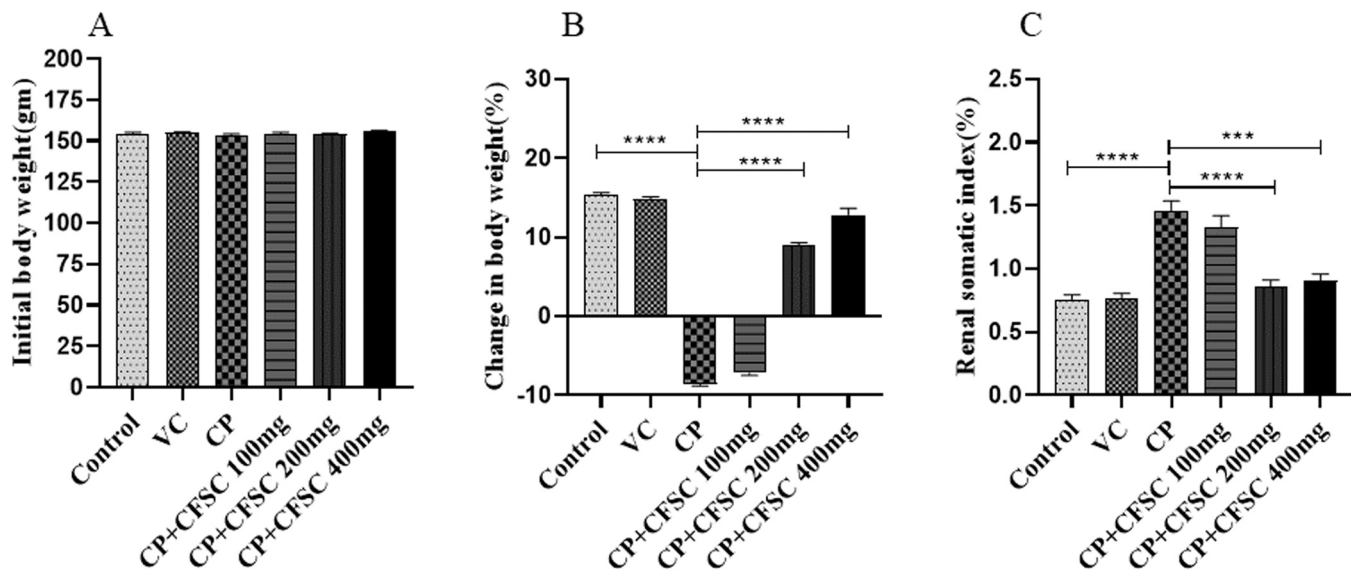


**Fig. 8.** Effect of CFSC on the initial body weight (A), body weight percentage (B), renal somatic index (C), of CP-induced AKI in rats. Data were expressed as Mean  $\pm$  SE (n = 6). Statistical analysis of two-way ANOVA followed by Tukey’s multiple comparison test were performed and significance level was tested at \*\*\* $p < 0.001$ , \*\*\*\* $p < 0.0001$ .

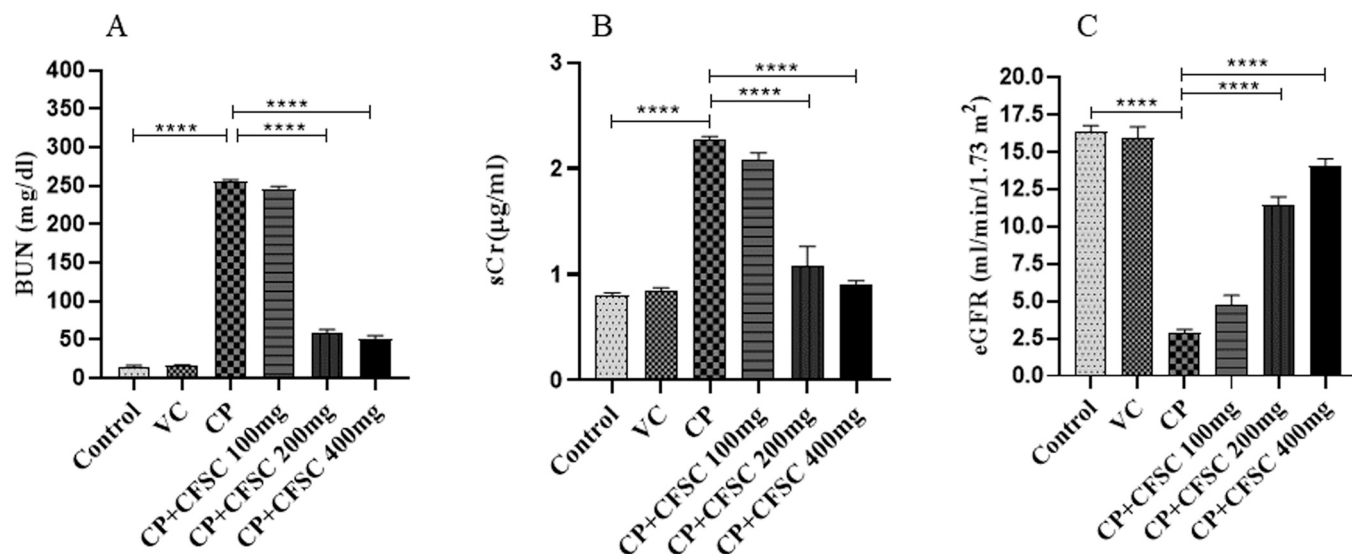


Fig. 9. Effect of CFSC on BUN (A) and sCr (B) and eGFR (C) in CP-induced AKI in rats. Data were expressed as Mean  $\pm$  SE (n = 6). Statistical analysis of two-way ANOVA followed by Tukey's multiple comparison test were performed and significance level was tested at \*\*\*\*p < 0.0001.

### 3.12. Effect of CFSC on the relative mRNA expression levels of kidney tissue on CP induced AKI in rats

According to Fig. 12(A-D), the mRNA expression of KIM-1, IL-18, Cys-C, and clusterin was significantly upregulated in the CP-induced group III animals when compared to the control group. In contrast, the mRNA was significantly ( $p < 0.05$ ) downregulated in the CFSC treated (200 mg and 400 mg/kg) animals. Furthermore, rats given CFSC orally at doses of 200 mg and 400 mg/kg bw for 15 days showed a marked upregulation in the mRNA expression of Bcl2 and Nrf2 in kidney tissues, whereas CP treated rats showed a significant ( $p < 0.05$ ) down-regulation in renal expression of Bcl2 and Nrf2 in comparison to the control group, but there were no changes observed in lower dose of CFSC, i.e. 100 mg/kg bw (group IV animals) (Fig. 12E & F). Similarly, the mRNA levels of HO-1 ( $P < 0.05$ ) and NQO-1 ( $P < 0.05$ ) are dramatically ( $P < 0.05$ ) decreased by CP-treatment, but this is reversed by high doses of CFSC (Fig. 12G & H). Additionally, qRT-PCR data represented that mRNA expression studies as a confirmatory analysis for KIM-1, IL-18, Nrf2, and Bcl2. When CP-treated group V and VI rats were

given 200 mg and 400 mg/kg bw of CFSC orally, their mRNA expression levels of KIM-1 and IL-18 were considerably ( $p < 0.05$ ) lower than those of CP-treated group III rats (Fig. 12I & J). When comparing the CP-induced AKI group to the control group, Fig. 12 (K-N) demonstrated a significant ( $p < 0.05$ ) down-regulation of the mRNA expression levels of Nrf2, Bcl-2, HO-1, and NQO1 in group III animals. In contrast to the CP-treated animals, rats given with CFSC orally at doses of 200 and 400 mg/kg bw for 15 days, there was a significant elevation in the mRNA expression of Nrf2, Bcl-2, HO-1, and NQO1 in kidney tissues.

### 3.13. Effect of CFSC on the relative protein expression levels of kidney tissue on CP-induced AKI

As seen in Fig. 13 (A-E), western blotting revealed that the kidney tissue of CP-induced group III rats had considerably ( $P < 0.05$ ) higher levels of KIM-1 and IL-18 and lower levels of Bcl2 and Nrf2 with compared to control. The CP-induced AKI rats treated with high doses (200 and 400 mg/kg bw) of CFSC showed a significant ( $p < 0.05$ ) downregulation and upregulation of both relative indicators' protein expression levels.

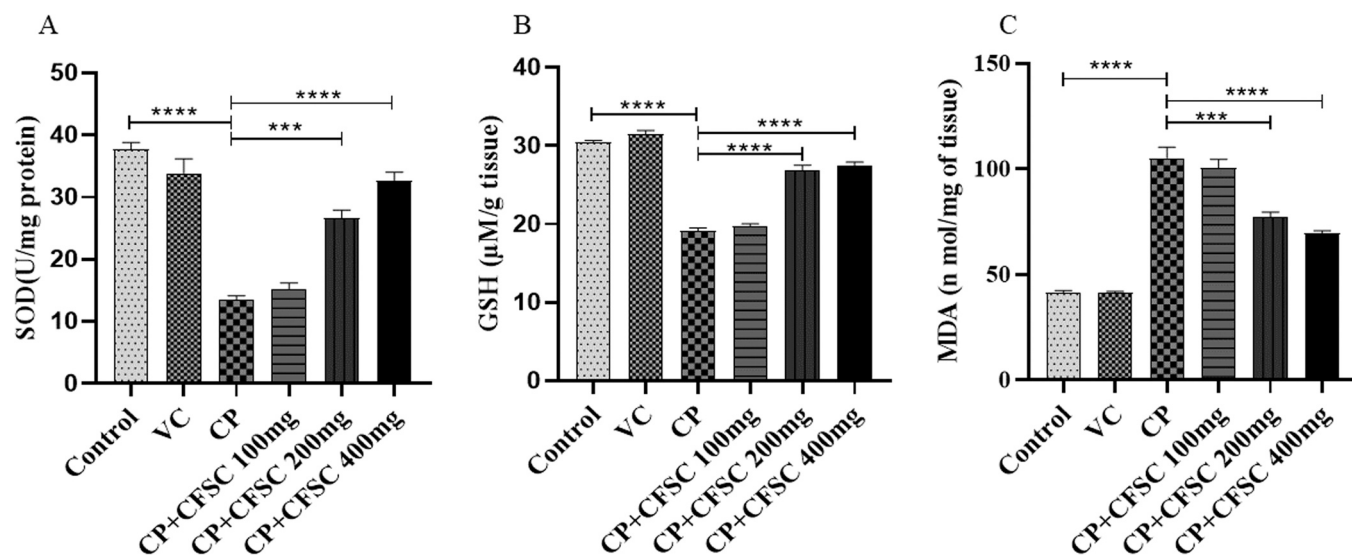
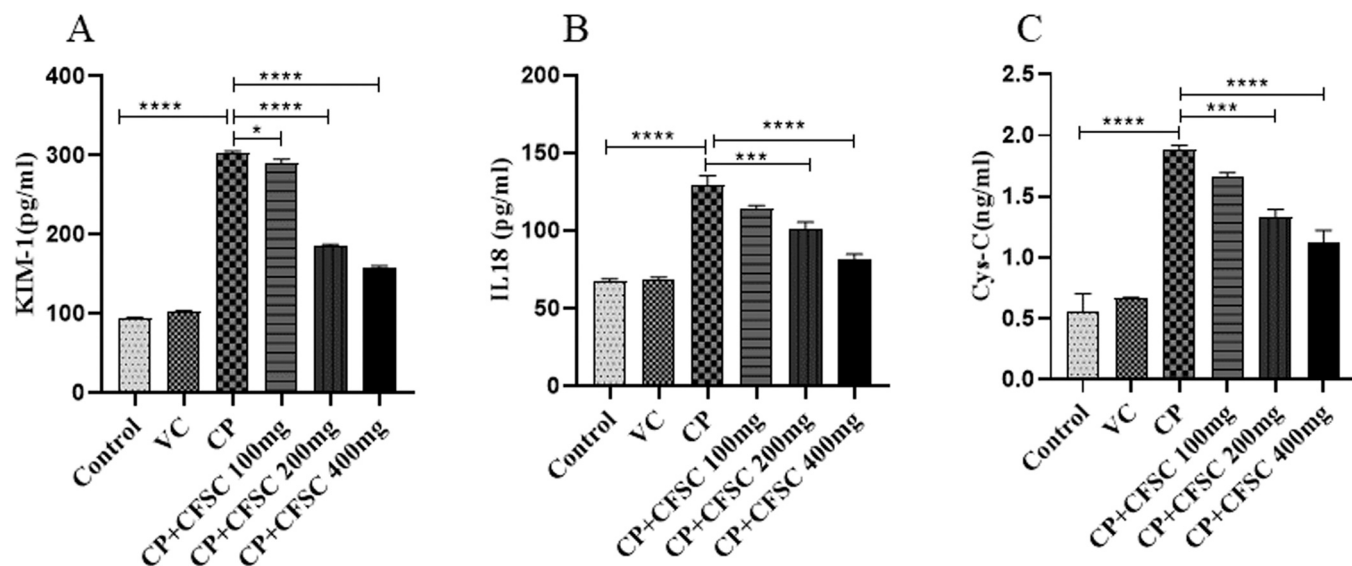


Fig. 10. Effect of CFSC on the levels of antioxidant SOD (A), GSH (B) & lipid peroxidation enzymes MDA (C) on CP-induced AKI in rats. Data were expressed as Mean  $\pm$  SE (n = 6). Statistical analysis of two-way ANOVA followed by Tukey's multiple comparison test were performed and significance level was tested at \*\*\*p < 0.001, \*\*\*\*p < 0.0001.



**Fig. 11.** Effect of CFSC on the urinary levels of KIM-1 (A), IL 18 (B) & Cys-C (C) in the CP-induced AKI in rats. Data were expressed as Mean  $\pm$  SE (n = 6). Statistical analysis of two-way ANOVA followed by Tukey's multiple comparison test were performed and significance level was tested at \*p < 0.05, \*\*\*p < 0.001, \*\*\*\*p < 0.0001.

### 3.14. CFSC improved renal pathological changes in CP-induced renal tissue damage

The renal tissues taken from the control and VC group (Fig. 14A & B) showed no histopathological damage, according to H&E examination. In comparison to the control group, rats treated with CP exhibited renal tubular lumen narrowing and some renal tubular epithelial cells displayed edema, degeneration, or necrosis (Fig. 14C). On the other hand, CFSC at 200 & 400 mg/kg bw reduced renal tissue damage and displayed a control-like histoarchitecture with intact glomeruli and tubules organized correctly (Fig. 14E & F), there was no significant changes observed in the CP treated animals orally fed with the lower doses of CFSC (100 mg/kg) (Fig. 14D). Animals treated with CP showed a significantly greater tubular injury score when compared to control. However high dosages of CFSC (200 & 400 mg/kg bw) were able to protect renal functions by preserving a normal histoarchitecture of kidney tissues, which resulted in a reduced injury score (Fig. 14G). The results of PAS staining also showed that the glomerulus, renal tubules, and renal interstitium were all well-organized in the control and vehicle control group of rats. The staining of the basement membrane showed complete integrity, and no abnormal alterations, including fibrosis and inflammatory cell infiltration, were found (Fig. 15A & B). In the animals in the CP-induced group the renal tubular lumen was abnormally dilated, the tubular epithelial cells' basement membrane staining was discontinuous, the epithelial cells were irregular and varied in size, there was more glycogen deposition, increased interstitial fibrosis, brush border loss, and glomerular hypertrophy (Fig. 15C & D). The similar observations were noted in the group IV animals treated with lower doses of CFSC. However, the tubular lesions were greatly alleviated by CFSC at doses of 200 & 400 mg/kg bw, which also preserved a normal brush boundary (black arrowhead) and little glycogen store in the basement membrane of renal cell (blue arrow) (Fig. 15E & F). Animals treated with CP showed a significantly greater glomerular injury score when compared to control (Fig. 15G).

### 3.15. CFSC reduces the extent of apoptosis in kidney tissue

In the current investigation, morphological analysis of DNA in kidney tissue was done by DAPI staining. DAPI staining, showed that cohesive and fragmented chromatin in nucleus, apoptotic cell deaths were clear apparent in the CP treated group. As shown in Fig. 16 (A-F),

CP-induced rats treated with CFSC at a lower dose of 100 mg/kg bw, the nuclear damage by CP was still evident, but with high doses of CFSC (200 & 400 mg/kg) there were increased number of live cells as DAPI does not stained to the healthy nucleus in the same concentrations. The average number of apoptotic cells was shown in Fig. 16G.

## 4. Discussion

*Sida cordifolia* L. (SC) is a medicinal plant that has been traditionally used for a variety of illnesses all over the world and as they contain a variety of bioactive compounds that are well-known for their biological effects, including the ability to scavenge free radicals, inhibit hydrolytic and oxidative enzymes, and reduce inflammation. The phenolic and flavonoid components found in CFSC are in extremely good quantities, and when compared to conventional vitamin C, the DPPH radical scavenging percentage of CFSC is also very high. The assay for DPPH radical scavenging is commonly utilized and favoured in the assessment of antioxidant activity. Since it is a free radical, the diamagnetic polymer of paraphenylamine can readily accept an electron or hydrogen from antioxidant molecules. The DPPH radical is thought to have a radical scavenging characteristic because of its capacity to bind H. The outcome of the DPPH scavenging activity indicates that CFSC includes a significant number of bioactive compounds that have the ability to give hydrogen to a free radical in order to eliminate the odd electron that causes the radical to be reactive [52]. In continuation, HPLC analysis of this specific fraction was compared using standard quercetin, glycitein and apigenin. The results indicate that similar peaks were observed in CFSC as compared with the standards. Quercetin, apigenin and glycitein are natural polyphenol, known to have antioxidant, anti-inflammatory, anti-microbial, and radical scavenging activities [45,53,54]. ESI-MS analysis of CFSC showed presence of many bioactive phytochemicals, out of which six major compounds were possibly present in abundant quantities that could have possessive potential nephroprotective properties. These are galangin, naringenin, (-)-Epiafzelechin, glycitein, 5,7-Dimethoxyflavanone and sakuranetin as results were matched with available ESI-MS library. These compounds were studied earlier by other researchers for their pharmacological properties mentioning in Table 3. Compounds identified by ESI-MS analysis, were studied by herb database and then selected as the potential candidates for network pharmacology analysis. All six compounds were screened the active ingredients using ADME simulation

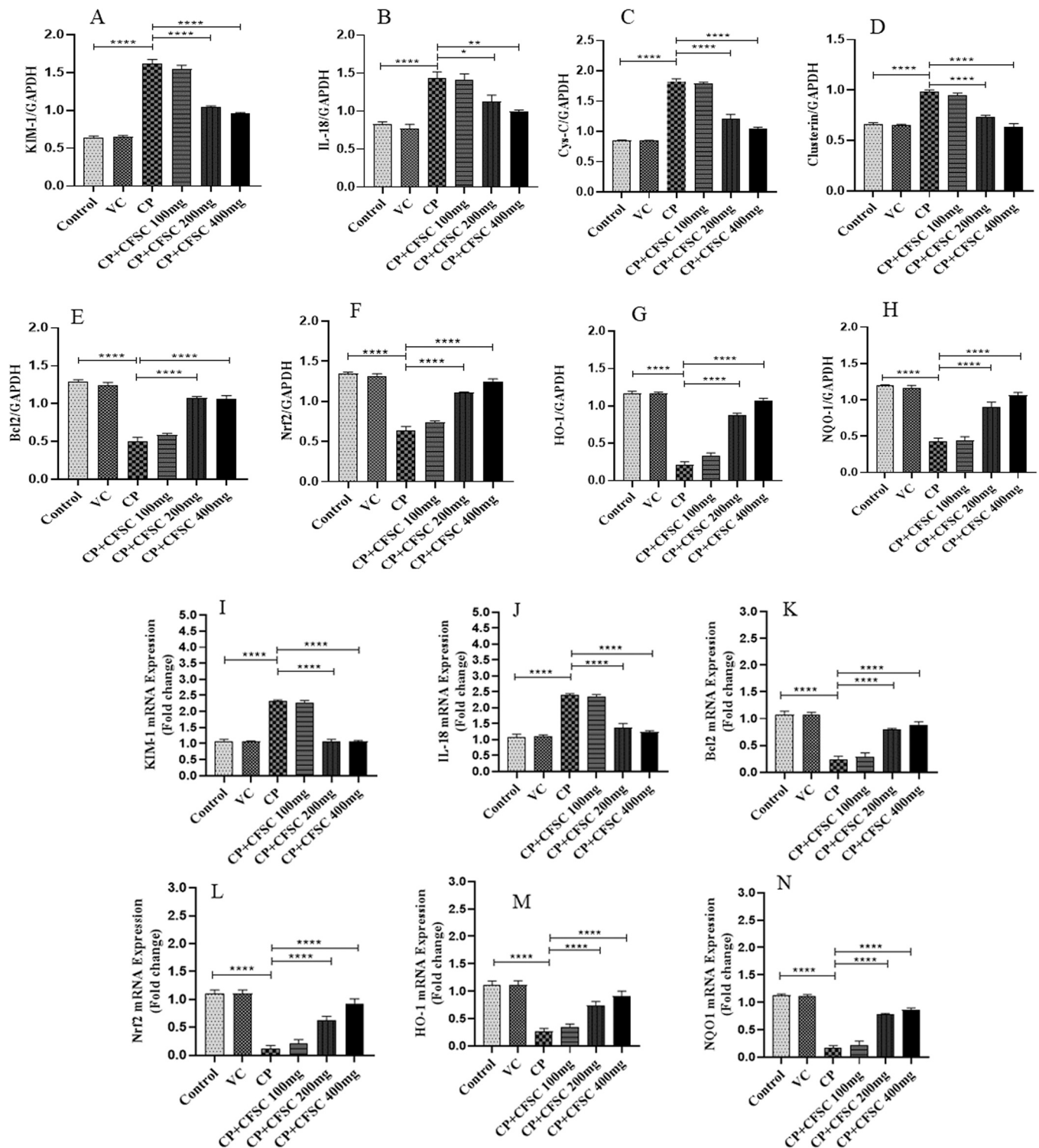


**Fig. 12.** The mRNA expression determined by semi q-PCR including KIM-1 (A), IL-18 (B), Cys-C (C), clusterin (D), Bcl-2 (E), Nrf2 (F), HO-1 (G) & NQO-1 (H) and qRT-PCR including KIM-1(I), IL-18 (J), Bcl-2 (K), Nrf2 (L), HO-1 (M) & NQO-1 (N) on CP-induced AKI in rats. Data were expressed as Mean  $\pm$  SE (n = 6). Statistical analysis of two-way ANOVA followed by Tukey's multiple comparison test were performed and significance level was tested at \*p < 0.05, \*\*p < 0.01, \*\*\*p < 0.0001.

parameters, especially the OB and DL parameters as the important evaluation indexes. Integrating the network topological parameters with all the network analyses, an exhibited that bioactive compounds of *Sida cordifolia* L., acted at multiple targets and multiple signalling pathways related to AKI. Then determined the hub targets of the active compounds, namely Bcl2, MAPK, ICAM-1 and others. These genes are associated with inflammation, and stress. Many studies confirmed that

inflammatory response and ECM deposition could be the crucial mechanistic pathways for developing renal fibrosis and hypoxia injury [55].

In NRK-52E cells, cisplatin caused alterations in normal cellular shape and an increase in cell death. CP and CFSC treated NRK-52E cells showed a marked increase in cell proliferation, suggesting that CFSC had cytoprotective properties against CP-induced cytotoxicity as

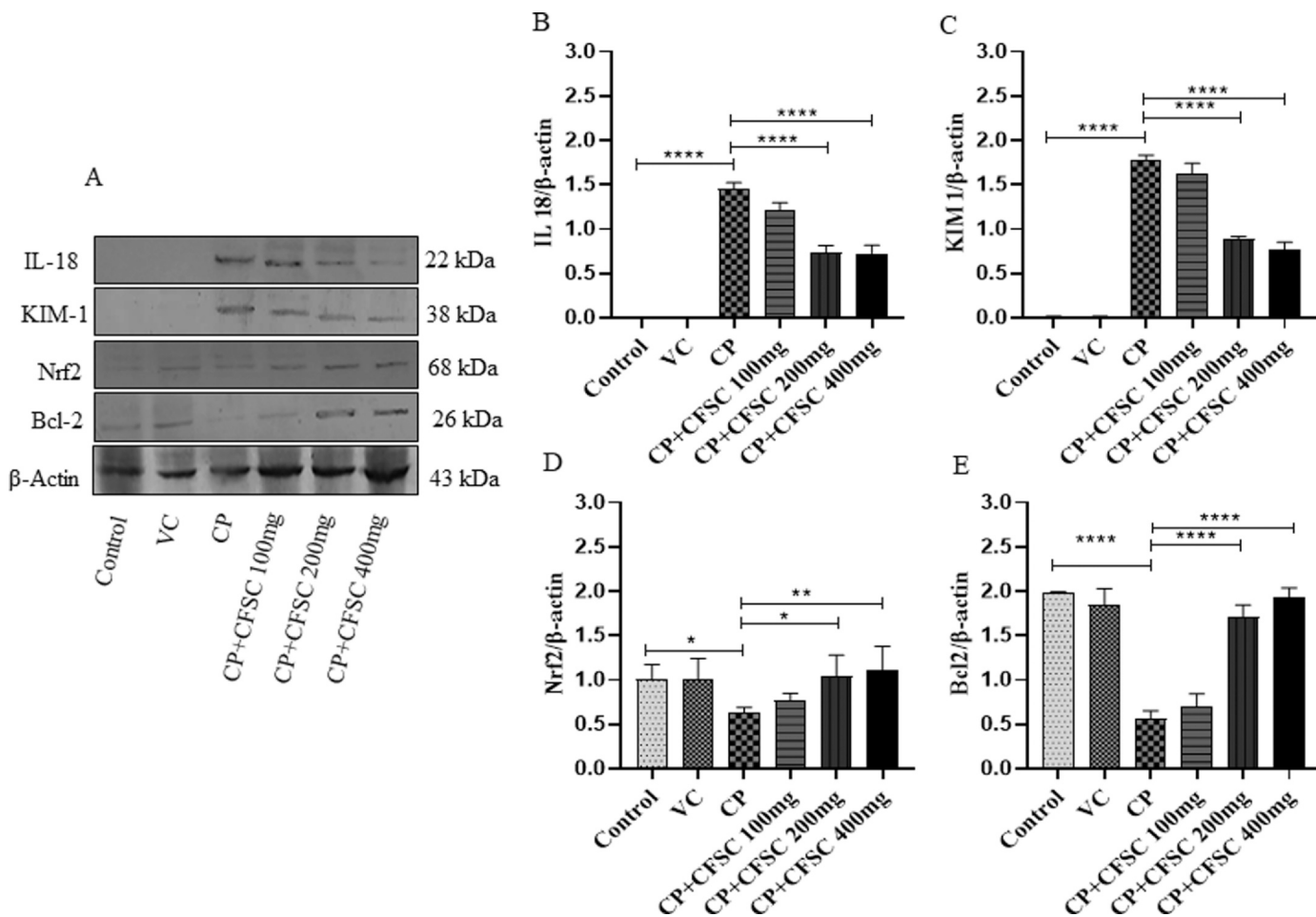


**Fig. 13.** The protein expression levels of , IL-18, KIM-1, Nrf2 & Bcl2 as determined by western blot on CP-induced AKI in rats (A-E). Data were expressed as Mean  $\pm$  SE (n = 6). Statistical analysis of two-way ANOVA followed by Tukey’s multiple comparison test were performed and significance level was tested at \*p < 0.05, \*\*p < 0.01, \*\*\*p < 0.0001.

studied via MTT assay [56]. Current findings demonstrated the protective function of CFSC in maintaining the vitality of CP-treated NRK-52E cells.

The membrane integrity of cells treated with CP was compromised, and the nucleus was stained with EB. In contrast, the essential dye AO can be used to stain the membranes of both living and dying cells, while EB can be used to identify cells with damaged membrane integrity. Normal, undamaged cells appear green, but cells in the early or late phases of apoptosis appear reddish-orange due to condensed and shattered nuclei. Necrotic cells will stain orange even if they have a normal nuclear structure and no condensed chromatin. NRK-52E cells going through apoptosis exhibit condensed chromatin and AO/EB dual staining, whereas healthy, live cells solely exhibit AO staining and appear green [57,58]. Current study reported that different doses of CFSC (50–200  $\mu$ g) could reduce CP-treated cell death and apoptosis, and increases anti-oxidant status due to presence of bioactive compounds [41,42].

Renal damage brought on by CP treatment lead to tubular cell death, tissue damage from the release of inflammatory cytokines, and a vicious cycle of oxidative stress and inflammatory reactions [35]. In this study, oral CFSC at high doses (200 and 400 mg/kg/day for 15 days) resulted in a significant drop in the renal somatic index and an increase in body weight in CP-treated AKI. The administration of CP to rats resulted in a notable decrease in body weight since the drug directly inhibits the breakdown of white adipose tissue by diminishing the amount of the white epididymal fat pad, a process that is accompanied by increased inflammation and cell death. This decrease could be

brought on by either tubular injury, which modifies water reabsorption and causes dehydration and loss of body weight, or the cytotoxic effects of CP on the gastrointestinal tract, which modify eating habits, disrupt gastrointestinal rhythm, and postpone gastric emptying, all of which contribute to weight loss in rats [59]. Increased glomerular volume and cellular degenerative changes, such as cytoplasmic vacuolization of the proximal tubular cells and tubular dilatation, are thought to be the causes of kidney disease indicated by an increase in renal somatic index [60]. CFSC contain many bioactive phytochemicals which may possess nephroprotective properties and thereby maintained a control like body weight and renal somatic index.

The majority of the time in clinical practice, the diagnosis of kidney injury is made using clinical markers like BUN and sCr, which are then supported by information on eGFR calculated using various equations that consider other factors such as age, gender, and race. The eGFR drop and a host of other physiological processes, including altered protein synthesis, loss of body weight or hunger, stomach or intestinal hemorrhage, and dehydration, can all have an impact on BUN and sCr levels [61]. Offerman et al. [62] state that in CP-induced nephrotoxicity in rats, renal vasoconstriction, decreased renal perfusion, and decreased glomerular hydrostatic pressure were the primary causes of the initial decline in GFR. Furthermore, current study reported that, sCr and BUN levels were not only significantly increased but also decreased eGFR was observed after CP treatment, but the levels of these uremic markers were settled to a normal level when rats were orally fed with CFSC at the high doses, as this plant could significantly improve the kidney damage caused by CP.

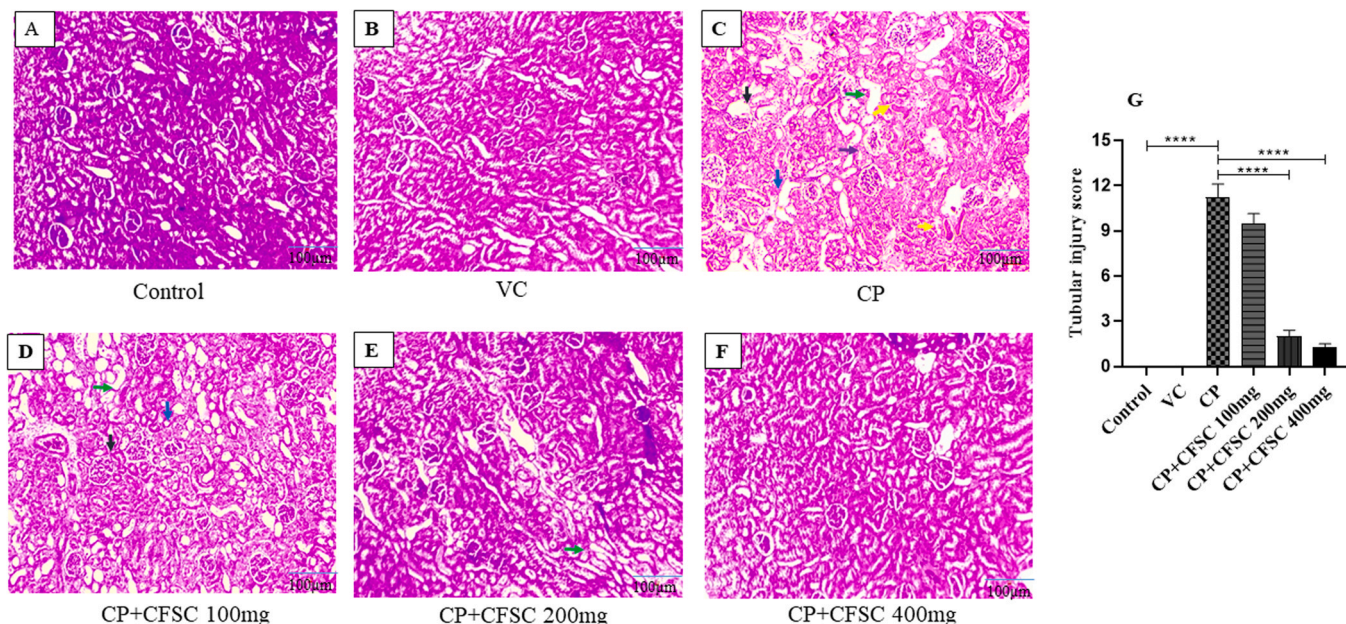


**Fig. 14.** Effect of CFSC on the histopathological changes of the kidney tissues of CP-induced AKI in rats. Slides were prepared using H&E staining and observed under (10X) (A-F). A and B: There were no alteration observed in the glomerular and tubular part of kidney tissues in control and vehicle control group. C: CP-induced AKI group showed glomerular hypertrophy (black arrow), renal tubular necrosis (blue arrow), presence of hyaline cast (Yellow arrow), increased tubular epithelial space (green arrow), thickening of glomerular basement membrane (purple arrow). D: CP-induced AKI animals orally fed with lower dose of CFSC (100 mg) does not provide nephroprotection thereby a similar histoarchitecture was observed with CP group. E & F: CP-induced AKI animals orally fed with high doses of CFSC (200 and 400 mg/kg) showed control like histoarchitecture, in which glomerular capillaries retain their normal size and appearance, and a slight renal tubular dilation was observed only in Fig. 14E (green arrow). G represented tubular injury score. Data were expressed as Mean ± SE (n = 6). Statistical analysis of two-way ANOVA followed by Tukey’s multiple comparison test were performed and significance level was tested at  $***p < 0.0001$ .

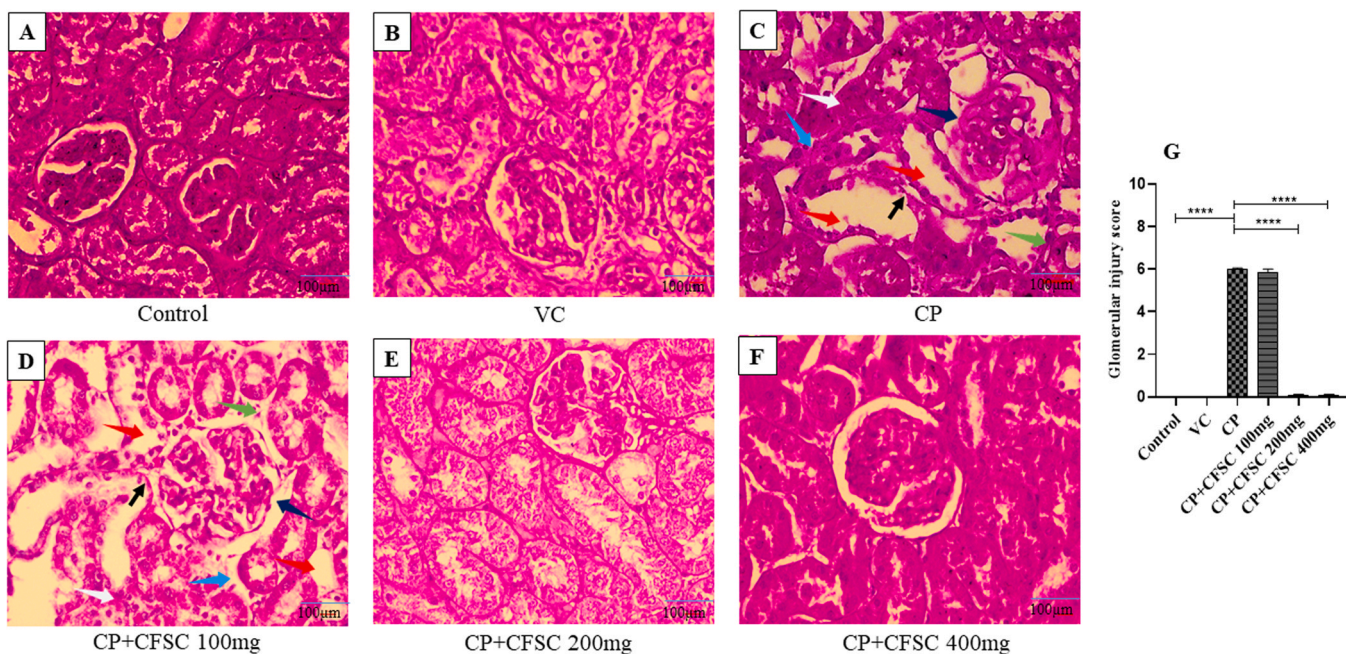


**Fig. 15.** Rats kidney tissue slices from the experimental animals at 40X magnification by PAS staining. PAS staining revealed that the morphological structure of the glomerulus capsule, renal tubular, and renal stroma were normal in the control group and vehicle group (A & B); the staining of the basement membrane demonstrated intact integrity, with no aberrant alterations like inflammatory cell infiltration and fibrosis were identified. In the CP treated group (C), the lumen of the renal tubules was abnormally dilated (red arrow); the hypertrophy of glomeruli (dark blue arrow), tubular epithelial cells had a discontinuous basement membrane (light blue arrow), and epithelial cells were different sizes and irregular (green arrow), accumulation of glycogen deposition (white arrow), also observed loss of brush border glycogen uptake (black arrow). There was no difference found between the CFSC treated at 100 mg/kg bw with CP group (D) and the CP-treated AKI group. High dosages of CFSC (200 and 400 mg/kg bw) administered to CP-induced rats (E & F) resulted in no obvious tubular lesions and a well-preserved histoarchitecture with intact glomerulus. G represented glomerular injury score. Data were expressed as Mean ± SE (n = 6). Statistical analysis of two-way ANOVA followed by Tukey’s multiple comparison test were performed and significance level was tested at  $***p < 0.0001$ .

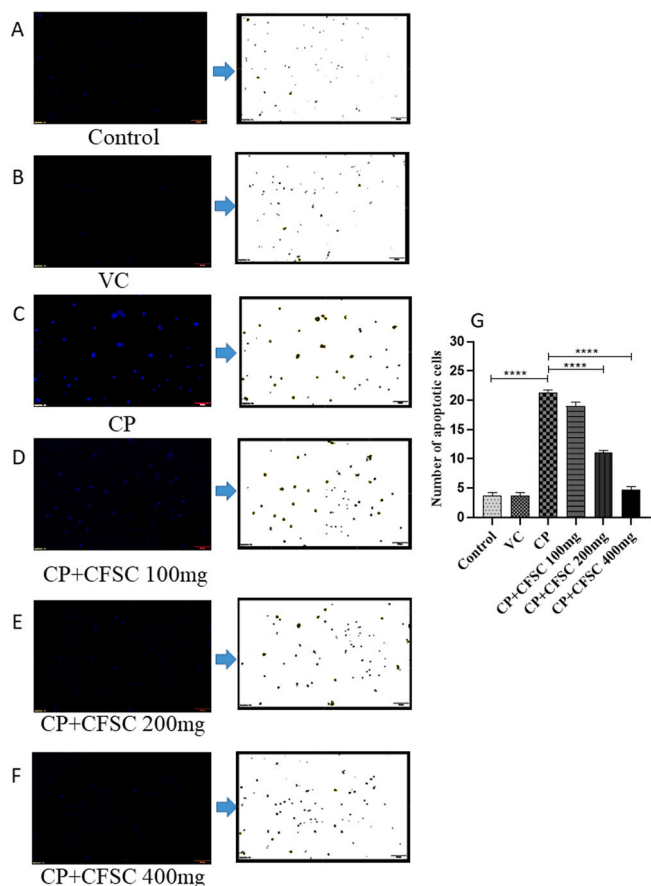


**Fig. 16.** Effect of CFSC on the nuclear DNA morphological changes of the kidney tissues of CP-induced AKI in rats. Slides were prepared using DAPI staining and observed under fluorescence microscope (10X) (A-F). G represented apoptotic cells counts. Data were expressed as Mean  $\pm$  SE (n = 6). Statistical analysis of two-way ANOVA followed by Tukey's multiple comparison test were performed and significance level was tested at \*\*\*\*p < 0.0001.

The main endogenous redox defensive mechanism against oxidative stress may be renal enzymatic and non-enzymatic antioxidant molecules. Research findings indicate that exposure to CP leads to an excess generation of free radicals, which in turn damages the kidneys through oxidative stress and lipid peroxidation. These reports demonstrated that CP compromised the kidneys' anti-oxidant defense mechanisms, which was followed by a marked drop in SOD and GSH levels and increased lipid peroxidation marker in the form of MDA level because of ROS production [63,64]. Numerous studies indicate, ROS causes histopathological alterations by reduction of GSH and SOD and formation of MDA and that has been linked to the pathophysiology of CP-induced AKI by directly acting on and destroying the structure of many cell components, including DNA, lipids, and proteins [65–67]. Naringenin was used in attenuating the level of SOD, GSH and decreased MDA in endoplasmic reticulum stress-induced renal cell death in hyperglycemic and diabetic renal toxicity [68,69]. Our results confirm that the substantial decreased in SOD and GSH levels following intraperitoneal injection of CP induced oxidative stress in kidney tissue. CFSC (200 and 400 mg/kg) was able to reduce oxidative stress brought on by CP via blocking the release of cytochrome-C and maintaining the membrane potential, which consequently raised SOD and GSH levels [69]. Similarly, the results of lipid peroxidation analysis showed that the expression level of MDA was higher in the CP treated group, and after CFSC co-administration (200 and 400 mg/kg), the expression level was lower which is similar to the control group. Our findings provide evidence that CFSC could restore its antioxidative status and reduced lipid peroxidation capacity due to presence of the bioactive compounds by

inhibiting oxidative stress related damage.

Previous studies have demonstrated a correlation between increased KIM-1 levels and inflammation [10], damage from ischemia, and different nephrotoxins, including CP [70]. Pro-inflammatory cytokines have been shown in numerous studies to play a crucial role in the pathophysiology of CP-induced kidney damage [71]. IL-18 is a sensitive and early indicator of renal tubular damage in the kidney [72,73]. A study found that among diabetic patients with normal albumin excretion, IL-18 was substantially linked to a reduction in eGFR. Since glomerular or tubular damage can eventually result in protein leakage, IL-18, an inflammatory biomarker, can predict the progression of renal injury caused by the presence of various cytotoxic drugs. As a result, elevated levels of IL-18 are strongly associated with the etiology of diabetic kidney disease, as well as AKI and CKD [74]. The urine of rats with CP-induced AKI contained soluble forms of KIM-1 and IL-18, which could be a valuable biomarker for inflammation and renal proximal tubular damage. Nonetheless, it was discovered that despite the large dosages of CFSC, KIM-1 and IL-18 levels in the urine were within normal ranges. In continuation, studies on related mRNA and protein expression, it was observed that both KIM-1 and IL-18 was significantly downregulated in the AKI rats orally fed with CFSC at high doses, and the lower dose of CFSC was ineffective to nephroprotection. The data suggested that CFSC significantly reduced the contents of inflammatory cytokines in serum and renal tissues of CP-induced rats and thereby suppressing inflammatory response [75,76]. According to a study, clusterin is intimately linked to renal disorders, particularly end-stage renal disease. In both human and animal models, polycystic kidney disease, ischemic renal tissues, and lupus-like nephritis are associated with increased expression of clusterin [77]. The detection of clusterin in urine is considered to be an exclusive indicator of damage to tubular epithelial cells by the CP-treated AKI model as clusterin is assumed to be unable to pass through the glomeruli and clusterin gene expression is known to be elevated in tubular injury [7,78]. Another kidney injury indicator linked to intracellular protein catabolism is Cys-C, a proteinase inhibitor. Circulating Cys-C often passes across the glomerular barrier without any problems. Megalin receptors allow Cys-C to be reabsorbed in the proximal tubules, where it undergoes complete metabolism. Because Cys-C is created at a highly constant rate, released into the plasma, and 99% of it is filtered by glomeruli, it is a useful biomarker of impaired renal function [79]. Numerous studies have demonstrated that serum and urine Cys-C levels are suitable indicators of tubular impairment, independent of eGFR and kidney disease markers that can be associated with inflammation [8,80]. Cys-C and clusterin in the kidney tissue was significantly downregulated to the CP treated rats receiving high doses of CFSC and demonstrated nephroprotective properties. This suggests that the plant compounds have a direct impact on reducing renal cell impairment and inflammation.

Cisplatin causes the pro-apoptotic gene Bax to become active. Bax then undergoes a conformational shift and binds to the mitochondrial membrane, which ultimately causes cytochrome C to be released and apoptosis to be triggered. On the other hand, cytochrome C release is blocked by the anti-apoptotic protein Bcl-2 via mitochondrial membrane stability. Since increased caspase 3 activity and abnormal expression of apoptosis-related proteins have been shown to play key roles in cells apoptosis, caspase 3 activity and apoptosis-related protein expression (Bcl-2 and Bax) were determined. Overexpression of Bcl-2 is associated with downregulate CP cytotoxicity [81–83]. When ROS are not adequately neutralized, they cause cell death and the deregulation of multiple signaling pathways, including Nrf2. In order to counteract elevated ROS, boosting the cellular antioxidant response has been a popular therapeutic strategy for cisplatin-induced AKI. Nrf2 is translocated to the nucleus, where it binds to AREr3 in the Bcl-2 gene's promoter region, increasing the gene's transcription. Increased Bcl-2 gene transcripts are translated into more Bcl-2 protein, which in turn causes a reduction in Bax, the release of cytochrome C, the activation of

caspace 3/7, a decrease in apoptosis, and an increased in cell survival. Through controlling the induction of a broad range of antioxidants and drug-metabolizing enzymes, such as SOD and GSH, Nrf2 has been linked to cellular antioxidant defenses and the preservation of redox homeostasis, according to subsequent research [84]. A deficit in Nrf2 increases a person's vulnerability to CP-induced nephrotoxicity, and Nrf2 may be crucial in preventing kidney damage. A network of enzymes that help counteract CP-induced oxidative damage by activating repair mechanisms to help combat the increased oxidative stress is ensured by the Nrf2 pathway, which is regulated by redox signalling. In early Nrf-2 over activation was found to protect cells from ROS damage and stop the progression of AKI to kidney diseases. Furthermore, the results of the present study demonstrated that the administration of CP resulted in a decrease in the levels of Bcl2 and Nrf2, while the oral feeding of CFSC at doses of 200 and 400 mg/kg markedly increased the expression of Bcl2 and Nrf2 as well as HO-1 and NQO1. This is due to the fact that CFSC has been demonstrated to enhance Nrf2 synthesis and Bcl2 activation in CP-induced AKI, both of which have been linked to the development of AKI and oxidative stress [85,86]. These findings suggest that the Nrf2/HO-1 and Bcl2 mediated pathway may be a useful target for treatment in AKI associated with oxidative stress. The CFSC contains natural bioactive phytochemicals like sakuranetin that enhance the activity of many key antioxidant enzymes. Both ameliorating effects of this fraction are associated with stimulate of antioxidants enzyme such as HO-1 and NQO-1. Previous study suggests that sakuranetin possesses of renal injury biomarkers, the mitigative potential to counteract microplastic prompted detrimental nephrotoxic effects via modulating the Nrf2/keap1, antioxidative and apoptotic genes expression [51]. The activation of Nrf2 ensuing release of HO-1 and NQO-1 having both antioxidant and anti-inflammatory actions [12]. A bioactive isoflavone treatment protected renal cell via inflammation against CP-treated renal inflammation through activation of the Nrf2 and its related gene expression of HO-1/NQO-1 signalling pathway.

Bencheikh et al. claim that the presence of toxic drugs results in aberrant changes in the kidney tissue, including a deplete in the number of cells in the glomeruli, vascular congestion, and loss of tubular constituents, that causes epithelial cell atrophy, distorting of the bowman capsule's epithelial cell membrane, and deformation of the bowman space. By enhancing the architecture of kidney tissue, polyphenols and flavonoids have been demonstrated to lessen the nephrotoxicity of

drugs; these findings are consistent with those of other authors [87]. In this study, CP-treated AKI rats exhibited vacuolar degenerative alterations of the tubular epithelium, as well as atrophy and infiltration of inflammatory cells, tubular dilatation, cellular infiltration, and extracellular matrix (ECM) deposition. The ability of tubular cells to adapt difficult conditions has been linked to the deposition of glycogen. The AKI rats in this study that received CP showed signs of ECM deposition in renal tissue, dilatation of tubular part, degenerative changes, and inflammatory infiltration of the tubules epithelial cell membrane. The histoarchitecture of the kidney tissues were intact with normal glomerular and renal tubular morphology, when CFSC was given orally in large doses at 200 and 400 mg/kg body weight. It can preserve the histological architecture of the kidney tissues with normal renal tubule appearance and typical glomeruli, and no specific injury was observed. DAPI staining indicated that treatment with CP causes increasing number of cells with condensed nuclei, as an indicator of dead cells, whereas the stain does not get penetrate into the healthy cells and thereby CFSC administration showed reduce visible cells in this staining, may be due to presence of many bioactive phytochemicals that are effective to prevents the nephrotoxicity caused by CP [88]. Our studies revealed that upregulation of Nrf2 and Bcl2 protein expression can able to protect CP-induced tubular damage as well as reduced accumulation of extracellular matrix by antioxidant activity of CFSC which may involve Nrf2 signalling pathway activation through IL-18 downregulation and activation of Nrf2-regulated genes such as NQO-1 and HO-1. Therefore, further studies related to the effects of CFSC on treatment of AKI and the possible mechanism by which therapeutic potential of this medicinal plant are needed to explore. Also clinical trial is essential in future to establish the proposed nephroprotective approach.

### 5. Conclusion

In conclusion, our findings demonstrate that CFSC can effectively provide nephroprotection and mitigate kidney damage resulting from CP-induced AKI. Furthermore, by activating the Nrf2 and Bcl2 mediated pathway and lowering the level of uremic biomarkers, inflammatory markers, oxidative stress, and renal fibrosis, the data suggest that the presence of bioactive phytochemicals in CFSC could contribute to controlling AKI (Fig. 17). Consequently, it is possible to draw the inference that *Sida cordifolia* L., may be a useful in the form of chloroform

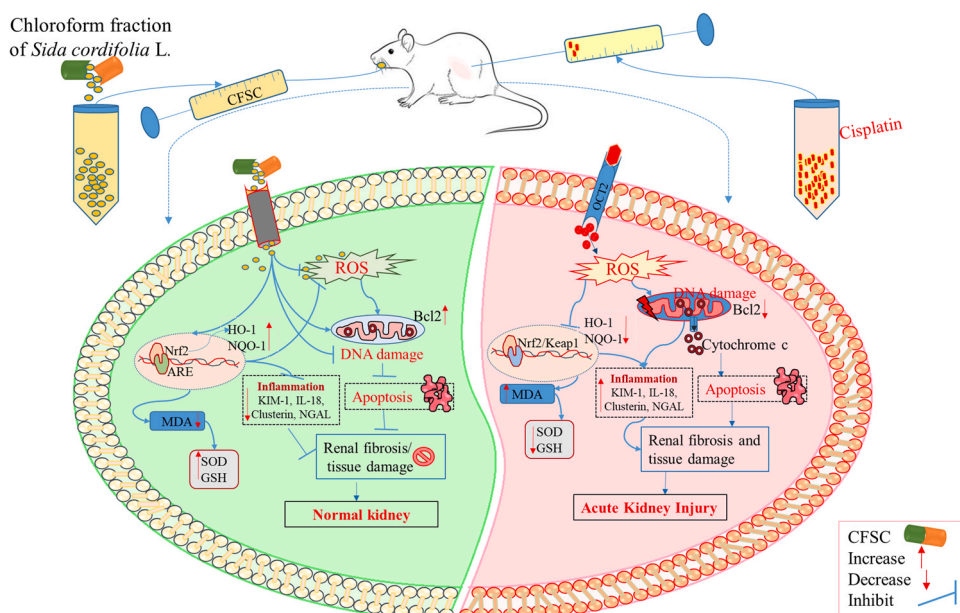


Fig. 17. Hypothetical overview of nephroprotective properties of CFSC against CP-induced acute kidney injury.

fraction for prevention of AKI and its associated complications, thus may offer an alternative approach to slow the progression of end stage renal diseases. In future, additional research on bioactive phyto-compounds of SC could have a significant impact on developing clinically effective measures for the patients suffering from kidney failure.

### CRedit authorship contribution statement

**Roy Suchismita:** Writing – review & editing, Writing – original draft, Visualization, Validation, Methodology, Investigation, Conceptualization. **Pradhan Shrabani:** Visualization, Validation, Formal analysis. **Das Pipika:** Methodology, Data curation. **Jana Sahadeb:** Writing – review & editing, Writing – original draft, Visualization, Validation, Supervision, Methodology. **Mitra Palash:** Writing – review & editing, Writing – original draft, Visualization, Validation, Investigation.

### Ethics Approval and Consent to Participate

This experiment was approved by the Institutional Animal Ethics Committee (IAEC) of Midnapore City College with the reference no-MCC/IAEC-SR/10/23–007, for the said experiment.

### Funding

This research did not receive any specific grant from funding agencies in the public, commercial, or not-for-profit sectors.

### Data availability

The data used to support the findings of this study will be made available from the corresponding author upon request.

### Declaration of Competing Interest

The authors declare that there are no conflicts of interest.

### Acknowledgements

The authors grateful to Dr. Pradip Ghosh, Director, Midnapore City College for essential support, a well-organized work environment and laboratory facilities for conducting related research work, the authors thankful to Mr. Souvik Roy, Bose institute, Kolkata, West Bengal, for facilities provided for ESI-MS analysis and ICMR, Govt. of India providing fund for HPLC and other expenses.

### References

- Al-Kuraishy H.M. Al-Gareeb A.I., (2021) Acute kidney injury and COVID-19. *Egyptian J. Int. Med.*, 33(1), 34.
- P. Vilela, L. Silva, WCN24-1271 social inequality in the prevalence of chronic kidney disease in Brazil, *Kidney Int. Rep.* 9 (4) (2024) S264–S265.
- X. Li, J. Shi, Y. Teng, Z. Liu, The preventative effect of Baihe Gujin Pill on cisplatin-induced acute kidney injury by activating the PI3K/AKT and suppressing the NF- $\kappa$ B/MAPK pathways, *J. Ethnopharmacol.* 318 (2024) 117071.
- C.Y. Fang, D.Y. Lou, L.Q. Zhou, J.C. Wang, B. Yang, Q.J. He, J.J. Wang, Q.J. Weng, Natural products: potential treatments for cisplatin-induced nephrotoxicity, *Acta Pharmacol. Sin.* 42 (2021) 1951–1969.
- H.M. Al-Kuraishy, A.I. Al-Gareeb, M.S. Al-Nami, Vinpocetine improves oxidative stress and pro-inflammatory mediators in acute kidney injury, *Int. J. Prev. Med.* 10 (2019) 142.
- H.M. Al-Kuraishy, A.I. Al-Gareeb, N.R. Hussien, Synergistic effect of berberine and pentoxifylline in attenuation of acute kidney injury, *Int. J. Crit. Illn. Inj. Sci.* 9 (2) (2019) 69–74.
- M.S. Al-Naimi, H.A. Rasheed, N.R. Hussien, H.M. Al-Kuraishy, A.I. Al-Gareeb, Nephrotoxicity: role and significance of renal biomarkers in the early detection of acute renal injury, *J. Adv. Pharm. Technol. Res.* 10 (3) (2019) 95–99, [https://doi.org/10.4103/japtr.JAPTR\\_336\\_18](https://doi.org/10.4103/japtr.JAPTR_336_18).
- S. Jana, P. Mitra, S. Roy, Proficient novel biomarkers guide early detection of acute kidney injury: a review, *Diseases* 11 (2022) 8.
- T. Jing, J. Liao, K. Shen, X. Chen, Z. Xu, W. Tian, Y. Wang, B. Jin, H. Pan, Protective effect of urolithin a on cisplatin-induced nephrotoxicity in mice via modulation of inflammation and oxidative stress, *Food Chem. Toxicol.* 129 (2019) 108–114.
- S. Jana, P. Mitra, T. Panchali, A. Khatun, T.K. Das, K. Ghosh, S. Pradhan, S. Chakrabarti, S. Roy, Evaluating anti-inflammatory and anti-oxidative potentialities of the chloroform fraction of *Asparagus racemosus* roots against cisplatin induced acute kidney injury, *J. Ethnopharmacol.* 339 (2025) 119084.
- M. Zdziechowska, A. Gluba-Brzózka, A.R. Poliwczak, B. Franczyk, M. Kidawa, M. Zielinska, J. Rysz, Serum NGAL, KIM-1, IL-18, L-FABP: new biomarkers in the diagnostics of acute kidney injury (AKI) following invasive cardiology procedures, *Int. Urol. Nephrol.* 52 (2020) 2135–2143.
- Y. Hao, J. Miao, W. Liu, L. Peng, Y. Chen, Q. Zhong, Formononetin protects against cisplatin-induced acute kidney injury through activation of the PPAR $\alpha$ /Nrf2/HO-1/NQO1 pathway, *Int. J. Mol. Med.* 47 (2021) 511–522.
- Q. Chen, H. Peng, L. Dong, L. Chen, X. Ma, Y. Peng, S. Dai, Q. Liu, Activation of the NRF2-ARE signalling pathway by the Lentinula edodes polysaccharose LNT alleviates ROS-mediated cisplatin nephrotoxicity, *Int. Immunopharmacol.* 36 (2016) 1–8.
- M.A. Ansari, Sinapic acid modulates Nrf2/HO-1 signaling pathway in cisplatin-induced nephrotoxicity in rats, *Biomed. Pharmacother.* 93 (2017) 646–653.
- P. Pila, P. Chuammitri, P. Patchanee, K. Pringproa, K. Piyarungsri, Evaluation of Bcl-2 as a marker for chronic kidney disease prediction in cats, *Front. Vet. Sci.* 9 (2023) 1043848.
- M.E. Mohamed, Y.S. Abduldaium, N.S. Younis, Ameliorative effect of linalool in cisplatin-induced nephrotoxicity: the role of HMGB1/TLR4/NF- $\kappa$ B and Nrf2/HO1 pathways, *Biomolecules* 10 (2020) 1488.
- S.M. Bagshaw, R. Bellomo, Cystatin C in acute kidney injury, *Curr. Opin. Crit. Care* 16 (2010) 533–539.
- K. Musiał, M. Augustynowicz, I. Miśkiewicz-Migoń, K. Kałwak, M. Ussowicz, D. Zwolińska, Clusterin as a new marker of kidney injury in children undergoing allogeneic hematopoietic stem cell transplantation—a pilot study, *J. Clin. Med.* 9 (2020) 2599.
- L. Zhang, L. Han, X. Wang, Y. Wei, J. Zheng, L. Zhao, X. Tong, Exploring the mechanisms underlying the therapeutic effect of *Salvia miltiorrhiza* in diabetic nephropathy using network pharmacology and molecular docking, *Biosci. Rep.* 41 (2021) BSR20203520.
- F. Noor, M. Tahir Ul Qamar, U.A. Ashfaq, A. Albutti, A.S.S. Alwashmi, M.A. Aljasir, Network pharmacology approach for medicinal plants: review and assessment, *Pharmaceuticals* 15 (2022) 572.
- V. Tiwari, S. Hemalatha, Sida cordifolia L. attenuates behavioral hypersensitivity by interfering with KIF17-NR2B signaling in rat model of neuropathic pain, *J. Ethnopharmacol.* 319 (2024) 117085.
- B. Dinda, N. Das, S. Dinda, M. Dinda, I. SilSarma, The genus *Sida* L. - a traditional medicine: its ethnopharmacological, phytochemical and pharmacological data for commercial exploitation in herbal drugs industry, *J. Ethnopharmacol.* 176 (2015) 135–176.
- H. Ahmed, A.S. Juraimi, M.K. Swamy, M.S. Ahmad-Hamdani, D. Omar, M.Y. Rafii, U.R. Sinniah, M.S. Akhtar, Botany, chemistry, and pharmaceutical significance of *Sida cordifolia*: a traditional medicinal plant, *Anticancer Plant Prop. Appl.* (2018) 517–537.
- R.S. Pawar, S. Kumar, F.A. Toppo, Lakshmi PK, P. Suryavanshi, *Sida cordifolia* Linn. accelerates wound healing process in type 2 diabetic rats, *J. Acute Med.* 6 (2016) 82–89.
- B. Joseph, A.U. Ajisha, S. Kumari, S. Sujatha, Effect of bioactive compounds and its pharmaceutical activities of *Sida cordifolia* (Linn.), *Int. J. Biol. Med. Res.* 2 (2011) 1038–1042.
- S. Kumar, P.K. Lakshmi, C. Sahi, R.S. Pawar, *Sida cordifolia* accelerates wound healing process delayed by dexamethasone in rats: effect on ROS and probable mechanism of action, *J. Ethnopharmacol.* 235 (2019) 279–292.
- H. Ahmed, A.S. Juraimi, M.K. Swamy, M.S. Ahmad-Hamdani, D. Omar, M.Y. Rafii, U.R. Sinniah, M.S. Akhtar, Botany, chemistry, and pharmaceutical significance of *Sida cordifolia*: a traditional medicinal plant, *Anticancer Plant. Prop. Appl.* (2018) 517–537.
- K. Wolfe, X. Wu, R.H. Liu, Antioxidant activity of apple peels, *J. Agric. Food Chem.* 51 (2003) 609–614.
- S. Roy, S.H. Pradhan, S.H. Mandal, K. Das, A.R. Patra, A.N. Samanta, B.A. Sinha, S. Kar, D.K. Nandi, Phytochemical analysis, antimicrobial activity and assessment of potential compounds by thin layer chromatography of ethanol fraction of *Asparagus racemosus* roots, *Int. J. Pharm. Pharm. Sci.* 6 (2014) 367–370.
- M.S. Sammani, S. Clavijo, A. Figuerola, V. Cerdà, 3D printed structure coated with C18 particles in an online flow system coupled to HPLC-DAD for the determination of flavonoids in citrus external peel, *Microchem. J.* 168 (2021) 106421.
- S. Mitra, N. Naskar, K. Ghosh, A. Dutta, S. Lahiri, P. Chaudhuri, A. Saha, Studies on radiation stability of natural caffeine, *Appl. Radiat. Isot.* 183 (2022) 110148.
- R. Lateef, P. Mandal, K.M. Ansari, M.J. Akhtar, M. Ahamed, Cytotoxicity and apoptosis induction of copper oxide-reduced graphene oxide nanocomposites in normal rat kidney cells, *J. King Saud. Univ. -Sci.* 35 (2023) 102513.
- M. Kpemissi, K. Metowogo, M. Melila, V.P. Veerapur, M. Negru, M. Tulescu, A.V. Potârniche, D.S. Suhas, T.A. Puneeth, S. Vijayakumar, K. Ekl-Gadegbeku, K. Aklidikou, Acute and subchronic oral toxicity assessments of *Combretum micranthum* (Combretaceae) in Wistar rats, *Toxicol. Rep.* 7 (2020) 162–168.
- D.L. Hickman, Minimal exposure times for irreversible euthanasia with carbon dioxide in mice and rats, *J. Am. Assoc. Lab. Anim. Sci.:* JAALAS 61 (3) (2022) 283–286.

- [35] S. Jana, P. Mitra, A. Dutta, A. Khatun, T. Kumar Das, S. Pradhan, D. Kumar Nandi, S. Roy, Early diagnostic biomarkers for acute kidney injury using cisplatin-induced nephrotoxicity in rat model, *Curr. Res Toxicol.* 5 (2023) 100135.
- [36] K.J. Livak, T.D. Schmittgen, Analysis of relative gene expression data using real-time quantitative PCR and the 2(-Delta Delta C(T)) Method, *Methods* 25 (2001) 402–408.
- [37] S. Stael, L.P. Miller, Á.D. Fernández-Fernández, F. Van Breusegem, Detection of damage-activated metacaspase activity by Western blot in plants, *Methods Mol. Biol.* 2447 (2022) 127–137.
- [38] W.Q. Li, J.Y. Wu, D.X. Xiang, S.L. Luo, X.B. Hu, T.T. Tang, T.L. Sun, X.Y. Liu, Micelles loaded with puerarin and modified with triphenylphosphonium cation possess mitochondrial targeting and demonstrate enhanced protective effect against isoprenaline-induced H9c2 cells apoptosis, *Int. J. Nanomed.* 14 (2019) 8345–8360.
- [39] T. Toprak, C.A. Sekerci, H.R. Aydın, M.A. Ramazanoglu, F.D. Arslan, B.I. Basok, H. Kucuk, H. Kocakogol, H.Z. Aksoy, S.S. Ascı, Y. Tamdır, Protective effect of chlorogenic acid on renal ischemia/reperfusion injury in rats, *Arch. Ital. di Urol. e Androl.* 92 (2) (2020).
- [40] Y.C. Huang, M.S. Tsai, P.C. Hsieh, J.H. Shih, T.S. Wang, Y.C. Wang, T.H. Lin, S.H. Wang, Galangin ameliorates cisplatin-induced nephrotoxicity by attenuating oxidative stress, inflammation and cell death in mice through inhibition of ERK and NF-kappaB signaling, *Toxicol. Appl. Pharmacol.* 329 (2017) 128–139.
- [41] Z. Calis, D. Dasdelen, A.K. Baltacı, R. Mogulkoc, Naringenin prevents renal injury in experimental hyperuricemia through suppressing xanthine oxidase, inflammation, apoptotic pathway, DNA damage, and activating antioxidant system, *Metab. Syndr. Relat. Disord.* 21 (2023) 275–281.
- [42] M.F. Khan, A. Mathur, V.K. Pandey, P. Kakkar, Naringenin alleviates hyperglycemia-induced renal toxicity by regulating activating transcription factor 4-C/EBP homologous protein mediated apoptosis, *J. Cell Commun. Signal* 16 (2022) 271–291.
- [43] A. Seccon, D.W. Rosa, R.A. Freitas, M.W. Biavatti, T.B. Creczynski-Pasa, Antioxidant activity and low cytotoxicity of extracts and isolated compounds from *Araucaria angustifolia* dead bark, *Redox Rep.* 15 (2010) 234–242.
- [44] D. Dey, N. Dey, S. Ghosh, N. Chandrasekaran, A. Mukherjee, J. Thomas, Potential combination therapy using twenty phytochemicals from twenty plants to prevent SARS-CoV-2 infection: an in silico approach, *Virusdisease* 32 (2021) 108–116.
- [45] J. Lei, L. Cao, Y. Li, Q. Kan, L. Yang, W. Dai, G. Liu, J. Fu, Y. Chen, Q. Huang, C.T. Ho, Y. Cao, L. Wen, Physiological evaluation and transcriptomic and proteomic analyses to reveal the anti-aging and reproduction-promoting mechanisms of glycitein in *Caenorhabditis elegans*, *Food Funct.* 15 (2024) 9849–9862.
- [46] Diksha, L. Singh, Glycitein prevents reserpine-induced depression and associated comorbidities in mice: modulation of lipid peroxidation and TNF- $\alpha$  levels, *Naunyn Schmiede Arch. Pharmacol.* 397 (2024) 6153–6163.
- [47] D.D. Orhan, E. Küpeli, E. Yesilada, F. Ergun, Anti-inflammatory and antinociceptive activity of flavonoids isolated from *Viscum album* ssp. *album*, *Z. Nat. C. J. Biosci.* 61 (2006) 26–30.
- [48] A. Palko-Labuz, E. Kostrzewa-Susłow, T. Janeczko, K. Środa-Pomianek, A. Poła, A. Uryga, K. Michalak, Cyclization of flavokawain B reduces its activity against human colon cancer cells, *Hum. Exp. Toxicol.* 39 (2020) 262–275.
- [49] D.E. Ali, R.A. El-Shiekh, M.A. El Sawy, A.A. Khalifa, S.S. Elblehi, N.H. Elsokkary, M.A. Ali, In vivo anti-gastric ulcer activity of 7-O-methyl aromadendrin and sakuranetin via mitigating inflammatory and oxidative stress trails, *J. Ethnopharmacol.* 335 (2024) 118617.
- [50] X. Deng, Y. Qu, M. Li, C. Wu, J. Dai, K. Wei, H. Xu, Sakuranetin reduces inflammation and chondrocyte dysfunction in osteoarthritis by inhibiting the PI3K/AKT/NF- $\kappa$ B pathway, *Biomed. Pharmacother.* 171 (2024) 116194.
- [51] A. Akbar, F. Amin, M. Batool, A. Khatoun, Z. Ahmad, U. Atique, Sakuranetin counteracts polyethylene microplastics induced nephrotoxic effects via modulation of Nrf2/Keap1 pathway, *J. King Saud. Univ. Sci.* 36 (2024) 103343.
- [52] K. Patel, S.R. Mangu, S.V. Sukhdeo, K. Sharan, Ethanolic extract from the root and leaf of *Sida cordifolia* promotes osteoblast activity and prevents ovariectomy-induced bone loss in mice, *Phytomedicine* 99 (2022) 154024.
- [53] Y. Wang, J. Fu, C. Zhang, H. Zhao, HPLC-DAD-ESI-MS analysis of flavonoids from leaves of different cultivars of sweet Osmanthus, *Molecules* 21 (2016) 1224.
- [54] P. Mitra, S. Jana, S. Roy, Insights into the therapeutic uses of plant derive phytochemicals on diabetic nephropathy, *Curr. Diabetes Rev.* 20 (2024) e230124225973.
- [55] M.J. Alqahtani, S.A. Mostafa, I.A. Hussein, S. Elhawary, F.A. Mokhtar, S. Albagami, M. Tomczyk, G.E. Batiha, W.A. Negm, Metabolic profiling of *Jasminum grandiflorum* L. flowers and protective role against cisplatin-induced nephrotoxicity: network pharmacology and in vivo validation, *Metabolites* 12 (2022) 792.
- [56] M. Ghasemi, T. Turnbull, S. Sebastian, I. Kempson, The MTT assay: utility, limitations, pitfalls, and interpretation in bulk and single-cell analysis, *Int. J. Mol. Sci.* 22 (2021) 12827.
- [57] C. Guo, H. Yuan, Z. He, Melamine causes apoptosis of rat kidney epithelial cell line (NRK-52e cells) via excessive intracellular ROS (reactive oxygen species) and the activation of p38 MAPK pathway, *Cell Biol. Int.* 36 (2012) 383–389.
- [58] X.L. Yuan, P. Zhang, X.M. Liu, Y.M. Du, X.D. Hou, S. Cheng, Z.F. Zhang, Cytological assessments and transcriptome profiling demonstrate that evodiamine inhibits growth and induces apoptosis in a renal carcinoma cell line, *Sci. Rep.* 7 (2017) 12572.
- [59] N. Al-Kharusi, H.A. Babiker, S. Al-Salam, M.I. Waly, A. Nemmar, I. Al-Lawati, J. Yasin, S. Beegam, B.H. Ali, Ellagic acid protects against cisplatin-induced nephrotoxicity in rats: a dose-dependent study, *Eur. Rev. Med. Pharmacol. Sci.* 17 (2013) 299–310.
- [60] S.Y. Saad, T.A. Najjar, M.O. Al-Sohaibani, The effect of rebamipide on cisplatin-induced nephrotoxicity in rats, *Pharmacol. Res.* 42 (2000) 81–86.
- [61] M. Perše, Ž. Večerić-Haler, Cisplatin-Induced rodent model of kidney injury: characteristics and challenges, *Biomed. Res. Int.* 2018 (2018) 1462802.
- [62] J.J. Offerman, S. Meijer, D.T. Sleijffer, N.H. Mulder, A.J. Donker, H.S. Kooops, G.K. van der Hem, Acute effects of cis-diamminedichloroplatinum (CDDP) on renal function, *Cancer Chemother. Pharmacol.* 12 (1984) 36–38.
- [63] M. Sabiullah, Estimation of serum creatinine, blood urea nitrogen and urine analysis in patients with diabetes to assess the renal impairments, *Int. J. Adv. Biochem. Res.* 3 (2019) 01–04.
- [64] I. Potočnjak, J. Marinić, L. Batičić, L. Šimić, D. Broznić, R. Domitrović, Aucubin administered by either oral or parenteral route protects against cisplatin-induced acute kidney injury in mice, *Food Chem. Toxicol.* 142 (2020) 111472.
- [65] J.Q. Wang, X.X. Liu, J.J. Zhang, C. Jiang, S.W. Zheng, Z. Wang, D.Y. Li, W. Li, D.F. Shi, Amelioration of cisplatin-induced kidney injury by arabinogalactan based on network pharmacology and molecular docking, *J. Funct. Foods* 104 (2023) 105504.
- [66] M.Y. Yehia, R.H. Mohamed, A. Ola, H. Manal, M. Tolba, M. Amina, Effect of cisplatin on the kidney of the albino rat and possible protective role of Vitamin C, *Med. J. Cairo Univ.* 87 (2019) 547–555.
- [67] K.R. McSweeney, L.K. Gadanec, T. Qaradakhı, B.A. Ali, A. Zulli, V. Apostolopoulos, Mechanisms of cisplatin-induced acute kidney injury: pathological mechanisms, pharmacological interventions, and genetic mitigations, *Cancers* 13 (2021) 1572.
- [68] Z. Calis, D. Dasdelen, A.K. Baltacı, R. Mogulkoc, Naringenin prevents renal injury in experimental hyperuricemia through suppressing xanthine oxidase, inflammation, apoptotic pathway, DNA damage, and activating antioxidant system, *Metab. Syndr. Relat. Disord.* 21 (2023) 275–281.
- [69] M.F. Khan, A. Mathur, V.K. Pandey, P. Kakkar, Naringenin alleviates hyperglycemia-induced renal toxicity by regulating activating transcription factor 4-C/EBP homologous protein mediated apoptosis, *J. Cell Commun. Signal* 16 (2022) 271–291.
- [70] J. Song, J. Yu, G.W. Prayogo, W. Cao, Y. Wu, Z. Jia, A. Zhang, Understanding kidney injury molecule 1: a novel immune factor in kidney pathophysiology, *Am. J. Transl. Res.* 11 (2019) 1219–1229.
- [71] Z.N. Ma, Y.Z. Li, W. Li, X.T. Yan, G. Yang, J. Zhang, L.C. Zhao, L.M. Yang, Nephroprotective effects of saponins from leaves of *Panax quinquefolius* against cisplatin-induced acute kidney injury, *Int. J. Mol. Sci.* 18 (2017) 1407.
- [72] J.M. Thomas, B.M. Huuskes, C.G. Sobey, G.R. Drummond, A. Vinh, The IL-18/IL-18R1 signalling axis: diagnostic and therapeutic potential in hypertension and chronic kidney disease, *Pharmacol. Ther.* 239 (2022) 108191.
- [73] D. Szumilas, A.J. Owczarek, A. Brzozowska, Z.I. Niemir, M. Olszanecka-Glinianowicz, J. Chudek, The value of urinary NGAL, KIM-1, and IL-18 Measurements in the early detection of kidney injury in oncologic patients treated with cisplatin-based chemotherapy, *Int. J. Mol. Sci.* 25 (2024) 1074.
- [74] Y. Nozaki, K. Kinoshita, T. Yano, K. Asato, T. Shiga, S. Hino, K. Niki, Y. Nagare, K. Kishimoto, H. Shimazu, M. Funaiuchi, I. Matsumura, Signaling through the interleukin-18 receptor  $\alpha$  attenuates inflammation in cisplatin-induced acute kidney injury, *Kidney Int.* 82 (2012) 892–902.
- [75] Q. Ren, F. Guo, S. Tao, R. Huang, L. Ma, P. Fu, Flavonoid fisetin alleviates kidney inflammation and apoptosis via inhibiting Src-mediated NF- $\kappa$ B p65 and MAPK signaling pathways in septic AKI mice, *Biomed. Pharmacother.* 122 (2020) 109772.
- [76] K. Al-Rubeaan, S.S. Nawaz, A.M. Youssef, M. Al Ghonaim, K. Siddiqui, IL-18, VCAM-1 and P-selectin as early biomarkers in normoalbuminuric Type 2 diabetes patients, *Biomark. Med.* 13 (2019) 467–478.
- [77] J.Y. Heo, J.E. Kim, Y. Dan, Y.W. Kim, J.Y. Kim, K.H. Cho, Y.K. Bae, S.S. Im, K.H. Liu, I.H. Song, J.R. Kim, I.K. Lee, S.Y. Park, Clusterin deficiency induces lipid accumulation and tissue damage in kidney, *J. Endocrinol.* 237 (2018) 175–191.
- [78] J. Guo, Q. Guan, X. Liu, H. Wang, M.E. Gleave, C.Y. Nguan, C. Du, Relationship of clusterin with renal inflammation and fibrosis after the recovery phase of ischemia-reperfusion injury, *BMC Nephrol.* 17 (2016) 133.
- [79] K. Nan-Ya, M. Kajihara, N. Kojima, M. Degawa, Usefulness of urinary kidney injury molecule-1 (Kim-1) as a biomarker for cisplatin-induced sub-chronic kidney injury, *J. Appl. Toxicol.* 35 (2015) 124–132.
- [80] A.M. Alhusaini, L.M. Fadda, I.H. Hasan, H.M. Ali, A. Badr, N. Elorabi, H. Alomar, Q. Alqahtani, E. Zakaria, A. Alanazi, Role of some natural anti-oxidants in the down regulation of Kim, VCAM1, Cystatin C protein expression in lead acetate-induced acute kidney injury, *Pharmacol. Rep.* 72 (2020) 360–367.
- [81] K. Soto, S. Coelho, B. Rodrigues, H. Martins, F. Frade, S. Lopes, L. Cunha, A.L. Papiola, P. Devarajan, Cystatin C as a marker of acute kidney injury in the emergency department, *Clin. J. Am. Soc. Nephrol.* 5 (2010) 1745–1754.
- [82] W. Li, J. Wu, J. Zhang, J. Wang, D. Xiang, S. Luo, J. Li, X. Liu, Puerarin-loaded PEG-PE micelles with enhanced anti-apoptotic effect and better pharmacokinetic profile, *Drug Deliv.* 25 (1) (2018) 827–837.
- [83] S.C. Borkan, The role of BCL-2 family members in acute kidney injury, *Semin Nephrol.* 36 (2016) 237–250.
- [84] S.K. Niture, A.K. Jaiswal, Nrf2 protein up-regulates antiapoptotic protein Bcl-2 and prevents cellular apoptosis, *J. Biol. Chem.* 287 (2012) 9873–9886.
- [85] B.G. Mapuskar, C.F. Pulliam, D. Zepeda-Orozco, B.R. Griffin, M. Furqan, D.R. Spitz, K.A. Allen, Redox regulation of Nrf2 in cisplatin-induced kidney injury, *Antioxidants* 12 (2023) 1728.
- [86] X. Fan, W. Wei, J. Huang, L. Peng, X. Ci, Daphnetin attenuated cisplatin-induced acute nephrotoxicity with enhancing antioxidant activity of cisplatin by upregulating SIRT1/SIRT6-Nrf2 pathway, *Front. Pharmacol.* 11 (2020) 579178.
- [87] N. Bencheikh, M. Bouhrim, L. Kharchoufa, O.M. Al Kamaly, H. Mechchate, I. Es-Safi, A. Dahmani, S. Ouahhoud, S. El Assri, B. Eto, M. Bnouham, M. Choukri, M. Elachouri, The nephroprotective effect of *Zizyphus lotus* L. (Desf.) fruits in a gentamicin-induced acute kidney injury model in rats: a biochemical and histopathological investigation, *Molecules* 26 (2021) 4806.
- [88] P. Majtnerová, T. Roušar, An overview of apoptosis assays detecting DNA fragmentation, *Mol. Biol. Rep.* 45 (2018) 1469–1478.